Report CR 114513

ADVANCED SOLID PROPELLANT MOTOR INSULATION

FINAL REPORT

by

P. L. Smith, Chemistry Supervisor
and
R. F. Russ, Senior Chemist
Propellant Development Department

July 1972

Prepared under Contract NAS2-6557 by

Aerojet Solid Propulsion Company
Sacramento, California

for

Ames Research Center
National Aeronautics and Space Administration

ABSTRACT

This program was directed toward the development of an advanced light-weight insulation system suitable for use in long duration, low pressure planetary orbiter-type motor applications. Experiments included the screening of various filler and binder materials with optimization studies combining the best of each. Small-scale test motor data were used to judge the degree of success.

GLOSSARY

CST	Castable, sprayable, trovelable
CTPB	Carboxyl-terminated polybutadiene
DER-332	Epoxide resin
DDI	Dimer diisocyanate
EPDM	Ethylene-propylene rubber
Gen-Gard V-44	Acrylonitrile butadiene insulation, General Tire & Rubber Company
Gen-Gard V-4030	EPDM insulation, General Tire & Rubber Company
HTPB	Hydroxyl-terminated polybutadiene
IBC-111	Castable insulation, Aerojet Solid Propulsion Company
IPDI	Isophoronediamine diisocyanate
LITE motor	Laboratory Insulation Test Evaluation motor
LD-124	Polybutylene glycol
MNA	Methyl Nadic Anhydride
NBR	Acrylonitrile butadiene rubber
PBAN	Polybutadiene acrylic acid acrylonitrile terpolymer
TDI	Tolylene diisocyanate
USR-3804	EPDM insulation, United States Rubber Company
WB-6320	Low-density, flexibilized phenolic impregnated silica cloth composite, Ferro Corporation

TABLE OF CONTENTS

FIGURE LIST

FIGURE LIST (cont.)

FIGURE LIST (cont.)

I. INTRODUCTION

This report presents the results of the Advanced Solid Propellant Motor Insulation Program. The work was conducted by Aerojet Solid Propulsion Company for the National Aeronautics and Space Administration Ames Research Center, under Contract NAS2-6557. The thirteen month program was initiated in July 1971 to develop an advanced light-weight insulation system suitable for space motor applications.

The primary technical emphasis in this work was directed toward improvement of thermal performance parameters of the insulation through improved ablation characteristics, specific gravity, and thermal conductivity.

II. SUMMARY

The Advanced Solid Propellant Motor Insulation Program was initiated in July 1971 under Contract NAS2-6557 to develop an advanced light-weight insulation for use in space motor applications.

Program effort was divided into five tasks.

Task 1 was a study to define the performance parameters for evaluation in laboratory tests. Task 2 was a laboratory evaluation effort to provide test data which will be assessed against the criteria defined in Task 1. The most promising candidate materials were tested in small-scale motors in Task 4, and based on the analysis of those results, a final insulation formulation was selected. In Task 3, installation techniques were developed for the selected material. Under Task 5, program reviews were prepared and presented to the NASA Technical Manager at the conclusion of Task 2 and during Task 4.

II. Summary (cont.)

Primary emphasis during the program was given to the understanding of the contributions made to overall insulation performance by the individual components. Extensive screening studies were conducted to optimize the types and concentration of various filler materials with thermosetting rubber mastic binders.

Five insulation formulations were tested for overall performance characteristics in small-scale test motors designed to simulate the full-scale motor operating environment. Two of the insulations were installed in a simulated full-scale motor.

A composite dual layer insulation was demonstrated to have achieved a weight performance of 1.6 times that of a commercially available insulation currently in use for space motor applications.

III. TECHNICAL DISCUSSION

A. PROGRAM OBJECTIVES

The basic objective of the ASPMI program was to advance the state-of-the-art of internal insulation applicable to low-thrust long-duration space craft propulsion systems. More specifically, the program objective was to develop a high performance, light-weight insulation significantly better than the industries standard Gen-Gard V-4030. To accomplish this task, goals were established for the critical insulation performance parameters. These goals are summarized as follows:

	Property	Goal
1.	Weight Performance	Twice as effective as Gen-Gard V-4030
2.	Specific Gravity	One-half or less than that of Gen-Gard V-4030
	or	
3.	Ablative Performance	Twice as effective as Gen-Gard V-4030
4.	Case Protection	Maximum case temperature during firing 366°K, maximum case temperature after firing 616°K
5.	Space Storability	Stable for minimum of 2 years
6.	Insulation Bond	Propellant limited, and 2 times propellant strength to case materials

Processing methods for the selected insulation must be amenable to normal in process quality control procedures.

B. TECHNICAL APPROACH

Two principal thermal mechanisms were considered to be the most important factors in the development of a light-weight internal insulation system. Thickness loss rate (Å) caused by propellant exhaust gases

III.B. Technical Approach (cont)

passing across the insulation surface and heat conduction are the two areas which required significant advances to achieve the program goals. The approaches utilized in formulating and laboratory performance testing are described below.

1. Materials

Two classes of materials were screened for possible use as light-weight internal insulation; those based on elastomeric binder systems and those utilizing hard, plastic, ablation-resistant matrices. The elastomeric insulations were further subdivided into calendered, vulcanizable insulation such as the Gen-Gard V-4030 and mastic thermo-setting rubbers.

Internal insulations are basically composed of solid fillers in a binder or matrix. Since the properties and performance of the insulation are influenced by both filler and matrix composition, the approaches to meeting the program goals involved separate consideration of the functions of each.

a. Matrices

The following characteristics were used in the selection of the insulation binder matrices.

Elongation - sufficient to withstand pressurization (case-expansion) and thermal cycling strains.

Char Characteristics - form stable char.

Thermal Stability - Retention of properties under high heat flux conditions.

Bond Compatibility - Strong stable bond to propellant.

III.B. Technical Approach (cont)

Specific Gravity - Low density binder system.

Processing Characteristics - Fabrication flexibility, good dimensional control.

The binders or polymers which were evaluated for the insulation matrix are listed below.

Elastomers		
Premolded	Mastic	Hard Plastic
EPR	CTPB	Phenolics
NBR	PBAN	
	HTPB	

All of the above listed materials have been used in rocket motor insulations. The elastomeric materials have all been characterized by good mechanical properties and processing characteristics with reasonably good char formations. The hard plastic materials have demonstrated outstanding char characteristics but are relatively rigid with high specific gravity.

b. Fillers

The selection of the proper fillers is critical to the performance of the insulation. The type and concentration of fillers govern the thermal conductivity and density of the insulation as well as the ablation characteristics. The density and thermal conductivity requirements of the program require the inclusion of gas in some form such as microballoons. Two other classes of fillers were included in the program; fibrous fillers were evaluated for char reinforcement and particulate fillers for flame retardation and transpirational cooling of the char layer.

III.B. Technical Approach (cont)

The fibers evaluated for the insulation are those which have demonstrated good ablation performance. Fibers serve to anchor the char to the substrate in the highly erosive atmosphere of the propellant gas stream. Those fibers evaluated include asbestos, refrasil, carbon, aluminum silicate and phenolic.

Particulate type fillers which were included in the program include ammonium salts, carbon black and antimony oxide. Materials such as ammonium salts were considered for their role as coolants. During thermal degradation, NH_3 and finally H_2 will evolve, serving to cool the char layer and reduce erosion rates. Salts selected must be stable under vacuum storage conditions.

Particular attention was given to the selection of fillers which would not absorb water. This approach was necessary to insure insulation compatibility with the propellant during long-term vacuum storage.

The effects of the various filler types alone and in combination with other fillers were studied to provide a basis for selecting the light-weight insulation.

2. Insulation Design

Two approaches were taken to provide an insulation system which would achieve the program goals. The first approach was to combine filler materials discussed above in optimized concentrations with a selected matrix to provide a homogeneous insulation. Careful optimization of the fillers in this system take advantage of the beneficial insulating characteristics of the material without suffering the degrading effects of the filler with respect to other properties of the insulation. For example, a high concentration of particulate filler in the

III.B. Technical Approach (cont)

insulation increases specific gravity without substantially improving ablative performance.

To ensure meeting the requirements of the program, it was necessary to consider the use of alternatives to a single, homogeneous insulation layer. It was considered advantageous to utilize a multi-layer system composed of two materials each designed to fulfill a specific function; for example, transpirational cooling, high char resistance, and low density and thermal conductivity.

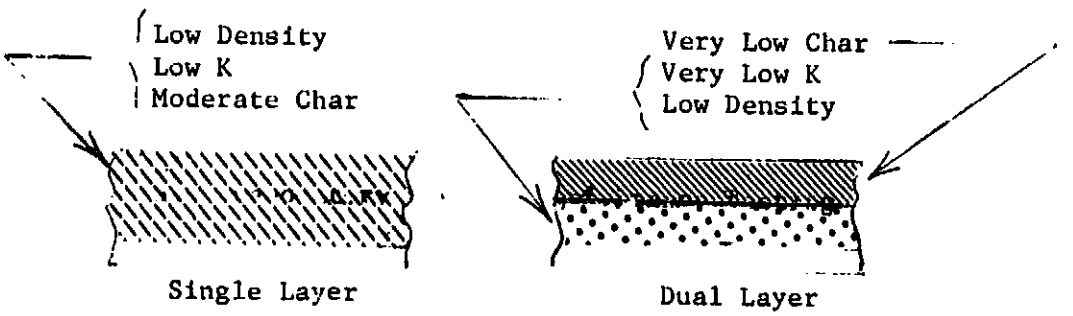

The dual layer concept appeared quite promising in that the insulation thickness requirements are dictated by the case temperature limitations as well as ablation rate. To satisfy the case temperature protection requirements a greater thickness of insulation is required than for simple ablative protection.

One obvious approach in using the dual layer concept was to use just enough Gen-Gard V-4030 to insure ablative protection over an inner layer of lightweight low thermal conductivity insulation which resulted in a composite insulation lighter in weight than all Gen-Gard V-4030. A second approach similar to the first in theory was to use the best experimental ablative insulation which would offer improved ablation characteristics and be lighter in weight than the

III.B. Technical Approach (cont.)

Gen-Gard V-4030, resulting in even greater weight savings than the first approach.

C. DISCUSSION OF RESULTS

The Advanced Solid Propellant Motor Insulation Program development work was organized into four major task efforts with one additional task designed to update the NASA Technical Director on the progress of the major task effort. A summary description of the elements of each task and their interrelationships is shown in Figure 1.

Task 1 was a study to define the performance parameters for evaluation in laboratory tests. Task 2 was a laboratory evaluation effort to provide test data which will be assessed against the criteria defined in Task 1. The most promising candidate materials were tested in small-scale motors in Task 4, and based on the analysis of those results, a final insulation formulation was selected. In Task 3, installation techniques were developed for the selected material. Under Task 5, program reviews were prepared and presented to the NASA Technical Manager at the conclusion of Task 2 and during Task 4.

1. Definition of Performance Parameters

The Task 1 effort consisted of the definition of critical performance parameters and establishment of criteria for rejection or continued evaluation of materials and/or concepts. The results are presented in Figure 2. The critical performance parameters defined include thermal performance characteristics for both single and dual layer insulation systems, bonding to propellant and to case materials, bond storage stability, mechanical properties, and space storability properties. In order to provide the necessary flexibility for evaluation, test, and selection of materials on the basis of overall performance; three sets of criteria were established for each critical performance parameter: (1) continue evaluation, (2) continue evaluation if warranted by overall performance potential, and (3) terminate evaluation.

III.C. Discussion of Results (cont.)

2. Laboratory Testing

Laboratory testing to evaluate the approaches selected for achievement of the program objectives was conducted in this task. A summary description of the elements of this task is shown diagramatically in Figure 3. Basically the task consisted of four elements: (1) Filler materials were screened using one basic elastomeric matrix PBAN and CTPB were found to be interchangeable and were used throughout this stage. Thermal performance characteristics, specific gravity and processing parameters were emphasized in the selection of fillers for additional testing. (2) Elastomeric matrix screening was conducted with selected filler combinations using the same performance parameters to judge the results. (3) Selected filler and mastic combinations were tested and compared to commercially available insulation. Primary emphasis in this element was achieving improvements in thermal performance and specific gravity. (4) Four candidate insulation systems were selected from the above screening tests and completely characterized with respect to all of the parameters outlined in Task 1.

To realistically assess the effects of insulation composition on thermal performance, a meaningful, low cost screening test was required. Commonly used screening tests involve directing a stream of hot gas from an oxyacetylene torch or plasma arc at the test specimen and measuring thickness loss rate, backside temperature rise, etc. The chief disadvantage of these tests is that the composition of the hot gas stream is entirely different from that of a propellant combustion gas and, consequently, good correlations of test data and motor firing performance were usually not obtained.

To provide a more realistic assessment, ASPC has developed a screening test comparable in cost to the plasma arc test but which uses solid propellant as the source of the hot gas stream. A schematic drawing of the test apparatus, termed Laboratory Insulation Test Evaluation (LITE), is shown in Figure 4. In operation, the secondary

III.C. Discussion of Results (cont.)

pressure vessel is initially pressurized with nitrogen to just under the desired operating pressure, and the propellant grain ignited. When the operating pressure is reached, the nitrogen input is regulated to provide steady state flow at the desired pressure (which is determined by the diameter of the outlet orifice). The duration of the test may be varied by using different propellant grain lengths. The mass flux through the cylindrical hole in the insulation test specimen may be controlled by selection of the hole diameter; for this program the environment to be simulated was an end-burning motor, and the test specimen hole diameter was made equal to the grain diameter.

The propellant used in the LITE motors is an unplasticized HTPB formulation containing 86 wt% total solids (18 wt% aluminum). A series of 4.5-Kg (10-lb) propellant batches were prepared to determine the correct oxidizer blend ratio to yield the target burning rate of approximately 0.51 cm/sec (0.2 in./sec) at 89.6 N/cm^2 (130 psia). Two blends (70/30 SSMP/MA and 70/30 unground/MA) were found to give the required burning rate (Figure 5) with good processing characteristics. Of the two, the SSMP/MA blend exhibited the lower viscosity, and 4.5-Kg(10-lb) batches of this propellant were prepared in order to make LITE motor grains to be used in the testing of insulation ablative properties. The LITE motor test set-up can accept a grain up to 17. cm (seven inches) (35 second duration), but screening tests were conducted with half-length grains.

The LITE motor test provided a very useful laboratory evaluation tool for realistic assessment of the effects of formulation parameters on the thermal performance of the advanced insulation materials developed on this program. To establish a basis for comparing the results of experimental test data, Figure 5 presents the ablation properties of Gen-Gard V-4030 along with other commercially available calendered insulations. An ablation rate of 0.076 mm/sec (3.0 mils/sec) was established as the characteristic ablation rate of Gen-Gard V-4030 for comparison with experimental test results.

III.C. Discussion of Results (cont.)

a. Filler Screening

(1) Microballoons

To achieve the program goals of a light-weight insulation material it was necessary to incorporate air into the insulation in a controlled reproducible manner. Aerojet has found that the only practical manner to accomplish this is through the use of microballoons. Other light-weight filler materials such as cork tend to permit absorption of the binder components into the cork, thus minimizing the effectiveness of the filler and reducing the capability of the binder to be loaded with other types of filler material.

Five types of microballoons were evaluated for use in both the single layer homogeneous insulation and the dual layer composite insulation concepts. Several types of microballoons were investigated on the basis of specific gravity, thermal performance and processing characteristics:

Microballoon Type	Chemical Composition	True Particle Specific Gravity	Mean Particle Diameter, Microns
IG-101	Borosilicate glass	0.34	76(1)
FTD-202	High-strength silica	0.28	53(1)
EC-SI	Silica	0.26	70(1)
A-200	Carbon	0.25	200(2)
UF-0	Urea-formaldehyde	0.24	30(2)

(1) Measured at ASPC using Micromerograph
(2) Estimated from manufacturer's data

III.C. Discussion of Results (cont.)

A series of 0.5-Kg (1-lb) batches of insulation were prepared with varying amounts of each of the above types of microballoon. As would be expected, the processability of the uncured mastic depended on both the concentration and true particle density of the microballoon since these determine the volume loading of filler. As shown by data in Figure 7, the higher density microballoons (such as IG-101) could be incorporated in higher concentrations, but the net result was that the insulation specific gravity was approximately the same at levels corresponding to equivalent processability. Insulation samples prepared in this study resulted in specific gravities of approximately 0.5-0.6 with adequate mixing and processing characteristics.

Since each of the different types of microballoons represent essentially a monomodal particle size distribution, the packing characteristics of the particles are probably not favorable for high filler loadings. The achievement of better particle packing was attempted through the use of a bimodal blend of particle sizes. The three types of glass microballoons were screened to remove the middle fraction (approx.) 40%. Batches prepared with a mixture of the remaining coarse and fine particles (2/1 ratio) showed some improvement in processing, but not enough to significantly increase the allowable solids loading. Based on theoretical considerations of packing density, the optimum size ratio of coarse to fine particles in a bimodal blend is approximately 10/1. The highest ratio that could be achieved in these screening experiments was only about 2/1 or 3/1.

Three microballoon types were selected for extensive thermal characterization in the CTPB mastic insulation; these were IG-101, FTD-202 and carbon spheres. The three types of microballoons represented the total spectrum in processing characteristics from the difficult to process carbon spheres to the more highly loaded IG-101 mastics. IG-101, the borosilicate glass microballoons showed superior thermal conductivity compared to both the carbon spheres and the FTD-202 (high strength silica) microballoons.

III.C. Discussion of Results (cont.)

Microballoon Type	Wt% in CTPB Mastic	Thermal Conductivity J/cm-sec-K°(BTU/ft-hr-°F)	
IG-101	35	0.073	(0.070)
FTD-202	35*	0.087	(0.084)
Carbon	25*	0.077	(0.074)

* Highest possible loading

Ablation tests conducted with samples containing various loadings of the three microballoons (Figure 8) indicate that the FTD-202 type is markedly superior to IG-101 and carbon spheres. The ablation rate for a CTPB mastic insulation is reduced approximately 25% from IG=101 when the FTD-202 was used. A 10% reduction in specific gravity is achieved with the use of FTD-202 in place of the IG-101 at the 35 wt% microballoon level. Observations of the mixing of insulation batches using the two microballoons tend to confirm the previously reported conclusion that the IG-101 was more processable than the FTD-202 material.

Based on density and ablation considerations the FTD-202 microballoon was selected for use in the combined filler evaluation described in a subsequent section.

However, the IG-101 microballoons were selected for use as the filler in the dual layer concept because of the improved thermal conductivity and the fact that ablation rate in the outer layer is of little significance.

(2) Fibers

Five types of fibrous fillers were evaluated in the CTPB or PBAN mastic binder systems. The fibers are shown below along with the specific gravity of each.

III.C. Discussion of Results (cont)

Fiber Name	Composition	Specific Gravity
Carbon	Carbon	1.84
Refrasil	Silica	2.32
Kynol	Phenolic	1.25
Kaowool	Aluminum Silicate	2.56
7TF-1	Asbestos	2.55

Four of the fibers were not usable in any practical way in the "as-received" state. The carbon and refrasil fibers had the appearance of coarse pieces of chopped yarn while the Kynol and Kaowool fibers were very long and intermingled. Attempts to incorporate 10 wt% fibers in a CTPB mastic binder resulted in very viscous non-homogeneous mixtures. Previous work had shown that processability of mastics containing fibers could be greatly improved if the fibers were reduced in size through some type of grinding process (wet or dry). Thermal performance of the materials was in general not affected. A quantity of eacn of the fibers was ground by passing a CTPB-fiber mixture through a three-roll paint mill. This process produced a much shorter fiber of very uniform size distribution as shown for the carbon fiber in the 40X photomicrograph of Figure 9. The Kynol fiber was significantly tougher than any of the other fibers and required a much longer grinding time to achieve the desired reduction in fiber length. All fibers processed well in formulations containing 30 wt% fiber, but the CTPB insulation formulation containing the Kynol and asbestos fibers did not cure. Satisfactory processing and cure were achieved with the PBAN mastic binder instead of the CTPB binder. The contribution of these fibrous fillers to thermal performance of the insulation was assessed using the 30 wt% filled mastics.

The effect of the fiber type on thermal conductivity is shown below.

III.C. Discussion of Results (cont)

Mastic	Fiber	Thermal Conductivity J/cm-sec-°K	(BTU/ft-hr-°F)
CTPB	Carbon	0.22	(0.21)
CTPB	Refrasil	0.16	(0.15)
CTPB	Kaowool	0.15	(0.14)
PBAN	Kynol	0.11	(0.11)
PBAN	Asbestos	0.18	(0.17)

* Fiber content of all samples 30 wt%.

The carbon fiber appears to impart a much higher thermal conductivity than the other fibers while Kynol fibers appear to be significantly lower.

Ablation rate measurements were made on mastics containing the same levels of fiber as used for the thermal conductivity tests. The test data (Figure 10) indicate the asbestos fiber to be the best fiber from the standpoint of ablation rate. To assess the effect of the mastic type on ablative performance, Kaowool fiber was prepared with each mastic. The measured ablation rate of the Kaowool-PBAN insulation was essentially identical to the Kaowool-CTPB insulation sample 0.117 and 0.119 mm/sec (4.6 and 4.7 mils/sec), respectively. The two samples showed similar weight losses indicating the mastic type had no influence on the comparison of the ablation properties of the five fibers.

From an overall performance standpoint the Kynol fiber appears to offer the greatest potential, however, processing characteristics and other problems with this fiber limit is usefulness. Both Kaowool and asbestos fibers demonstrated excellent processing qualities. Evaluation of all three fibers was continued in the combined filler work.

(3) Particulate Fillers

Primary emphasis in the evaluation of particulate fillers was placed on the ammonium salts. Ammonium sulfate has

III.C. Discussion of Results (cont)

been used as an exhaust coolant in propellant for some years. As shown in the tabulation below the ammonium salts offer significant improvements in specific gravity over commonly used fillers such as antimony oxide.

Particulate Filler	Specific Gravity
Ammonium Sulfate - $(NH_4)_2SO_4$	1.77
Ammonium Benzoate - $NH_4C_7H_5O_2$	1.28
Ammonium Citrate - $(NH_4)_2C_6H_5O_7$	1.48
Ammonium Phosphate, Monobasic - $NH_4H_2PO_4$	1.80
Ammonium Phosphate, Dibasic - $(NH_4)_2HPO_4$	1.63
Antimony Oxide - Sb_2O_3	5.67
Carbon - C	1.87

Three levels of $(NH_4)_2SO_4$ were evaluated in a CTPB mastic. Figure 11 indicates that $(NH_4)_2SO_4$ provides outstanding ablation properties over the entire range tested. Crushed and ground Micarta (paper reinforced phenolic) was also tested as a particulate filler. Processing the ground Micarta was very difficult and resulted in a maximum loading of only 30 wt% in the CTPB mastic. The ablation rate of a sample containing 30 wt% Micarta is also shown in Figure 11. The Micarta filled mastic did not provide improved ablation properties over the $(NH_4)_2SO_4$ sample of similar specific gravity. Gas cracks were characteristic of both the $(NH_4)_2SO_4$ and Micarta test samples. Therefore, additional evaluation of the particulate fillers were conducted using a combined filler insulation system. Additional tests using the ammonium salts with other fillers in combined insulation systems are discussed in the next section of this report.

b. Combined Filler Optimization

Three fillers were selected for initial testing of the combined filler system. Ammonium sulfate and FTD-202 microballoons were the

III.C. Discussion of Results (cont)

obvious choice in their respective categories. Kaowool fiber was selected for the initial phase of the combined filler testing.

Several combinations of filler levels were screened and are shown in Figure 12. These data may be compared with test results for Gen-Gard V-4030 and other commercially available insulations in Figure 6. Excellent ablation characteristics resulted from these combined fillers. Of particular note is the combination of 30 wt% $(NH_4)_2SO_4$, 10 wt% Kaowool and 20 wt% FTD-202 microballoons, the low ablation rate is coupled with a significant reduction in specific gravity. Observation of the tested samples indicated conditions of the char layer to be extremely good with a very tough bond between char and virgin material. The sample containing 35 wt% $(NH_4)_2SO_4$, 10 wt% Kaowool and 15 wt% FTD-202 resulted in similar ablation rates but with improved processability. This basic formulation was used to make fiber and particulate filler substitutions.

Ammonium benzoate, $NH_4C_7H_5O_2$, (30% less dense than ammonium sulfate) was substituted for ammonium sulfate to help reduce insulation weight. Asbestos and Kynol fibers were substituted for the Kaowool fiber. Figure 13 shows the results of these substitutions on the insulation ablation properties. The replacement of ammonium sulfate (a high gas producting particulate filler) with ammonium benzoate resulted in significant reductions in ablation rate with the Kaowool and asbestos fibers. The use of ammonium benzoate appeared to offer real advantages in reducing insulation weight as well as improving ablation properties, compared to the LITE motor results for Gen-Gard V-4030 (Figure 6).

In addition to the ammonium benzoate three other ammonium salts were tested in the basic combined filler formulation. Ammonium citrate, mono- and dibasic ammonium phosphates each gave ablation rates similar to ammonium sulfate but not as good as the ammonium benzoate. Figure 14 shows the LITE motor test results for these salts.

III.C. Discussion of Results (cont)

c. Binder Matrix Screening

Binder matrix screening tests were conducted using a filler combination consisting of 35 wt% $(NH_4)_2SO_4$, 10 wt% Kaowool and 15 wt% FTD-202 for the mastic type binder systems. Figure 15 shows a comparison of the various matrices evaluated in LITE motor tests. Four basic mastic polymers were used; (1) carboxyl-terminated polybutadiene (CTPB), cured with an epoxide-anhydride system; (2) polybutadiene, acrylic acid acrylonitrile terpolymer (PBAN), cured with an epoxide-anhydride system; (3) hydroxyl-terminated polybutadiene (HTPB), cured with diisocyanates; and (4) saturated hydroxyl-terminated polybutadiene (sat. HTPB) cured with diisocyanates. The two HTPB polymers were cured with toluene diisocyanate (TDI) and dimer diisocyanate (DDI).

LITE motor test data (Figure 15) indicate very little difference between the CTPB and PBAN polymers confirming the earlier finding with the fiber screening tests. The LITE motor test data obtained for the HTPB and saturated HTPB polymer systems showed inferior ablation rates for these systems compared to either CTPB or PBAN. Processing of the HTPB and saturated HTPB system showed a considerable variation in cure and potlife making these polymers very difficult to work with in obtaining good test specimens.

Samples of a calendered rubber stock prepared from ethylene-propylene-diene monomer (EPDM) at Kirkhill Rubber Company containing 20 wt% IG-101 microballoons were also evaluated in LITE motor tests.

The first rubber sample was not compounded with the cure accelerators and therefore could not be properly cured at ASPC. The partially cured rubber sample was bonded into a LITE motor insulation tube and tested. The ablation rate obtained (Figure 15), 0.091 mm/sec (3.6 mils/sec), was surprisingly good. A sample of the Gen-Gard V-4030 formulation rubber loaded with 20 wt% IG-101 was compounded at Kirkhill and tested in a similar

III.C. Discussion of Results (cont)

manner. There appears to be no effect of the curatives or ablation rate as the same rate 0.091 mm/sec (3.6 mils/sec) was obtained on this sample. The specific gravity obtained for this sample indicates the microballoon filler is being crushed to a considerable degree. With no crushing the specific gravity should have been 0.76 well below the 0.97 shown for the V-4030/IG-101 combination. This technique for lowering the specific gravity of a calendered rubber stock was therefore abandoned.

d. Silica Reinforced Phenolic

One of the most promising commercial insulation materials from the standpoint of thermal performance (based on technical data sheet information) was a phenolic impregnated silica fabric designated WB-6320.* This material uses microballoon filler in the phenolic resin to provide low density along with excellent thermal performance, and was of primary interest to this program as the inner layer of a composite insulation system. However, the cured insulation is a very hard material, and the first step in establishing its acceptabibility for use was determination of the insulation strain capability.

The biaxial strain capability of the cured insulation was measured in three directions relative to the weave direction of the fabric: (1) parallel to the weave, (2) perpendicular to the weave (parallel to the fill), and (3) on a 45° bias. The specimens consisted of three plies cured at 450°K (350°F) for 3.5 hours under a pressure of 10.3 N/cm^2 (15 psig). The data (Figure 16) indicate that the strain capability in the weave direction and on the bias is adequate (>8%), but parallel to the fill direction the elongation was only 1.1%. A minimum of 2% elongation was considered to be necessary to warrant continued evaluation of an insulation. Since the strain in the bias direction was satisfactory, additional specimens were prepared for testing consisting of six plies with each ply having the weave direction oriented 90 degrees with respect to the adjacent ply. These specimens were tested at both

* Ferro Corporation (Culver City, California)

III.C. Discussion of Results (cont)

low and high strain rates at zero degrees Fahrenheit (the most severe conditions). The data (Figure 16) show a minimum of 2.4% elongation.

These evaluations represent a very severe test of the insulation strain capability since edge effects in the biaxial specimen used tend to initiate failures via a tear mechanism which is not representative of the motor environment. Even so, the properties of the material appear sufficiently good to warrant further investigation. A LITE motor test was conducted with the WB-6320 material. The test results obtained were disappointing. Measurements indicated the entire sample thickness had charred resulting in an ablation rate of greater than 0.163 mm/sec (6.6 mils/sec). Since this material was being considered for use as the inner layer (low ablative) material no further tests were conducted.

e. Candidate Insulation Selection

Based on an analysis of the data discussed above, four candidate insulation systems were selected for the Task 3 and Task 4 scaleup, fabircation, and subscale motor testing phases. The four candidate insulation systems selected are summarized in Figure 17. They are: (1) IBT-121, a PBAN mastic with 10 wt% asbestos fiber, 35 wt% $(NH_4)_2SO_4$, 15 wt% FTD-202, (2) IBT-122, a PBAN mastic with 10 wt% asbestos fiber, 35 wt% ammonium benzoate, 15 wt% FTD-202, (3) dual layer system using IBT-123, a PBAN mastic with 35 wt% IG-101 microballoon filled outer layer and IBT-121 inner layer, and (4) dual layer system IBT-123 outer layer and Gen-Gard V-4030 inner layer. Based on the Task 2 laboratory testing data, these candidates had the potential for a weight performance up to 1.8 times that of the control Gen-Gard V-4030.

The PBAN mastic binder system was selected over the CTPB binder system based on greater flexibility in formulating to optimize the mechanical properties and allow the selection of the asbestos fiber for use in conjunction with ammonium benzoate. Even with the greater range in

III.C. Discussion of Results (cont)

formulating capability using the PBAN mastic, work with the ammonium benzoate filled insulation system was hampered by variability in the cure. For this reason additional filler screening tests were conducted during the Task 4 small-scale motor evaluation of the four selected candidates.

A new filler material was found during the Task 4 effort which exhibited an ablation rate equivalent to the best materials previously tested (ammonium benzoate) but without the cure and stability problems inherent with the ammonium benzoate. This material, hexamethylene tetramine (HMT), was used in a 1-to-1 mixture with ammonium sulfate at 17.5 wt% each, 15% FTD-202 microballoons, 10% 7TF1 asbestos, and 4 wt% PBAN binder. This system, IBT-124, had an average measured (LITE motor) ablation rate of 0.056 mm/sec (2.4 mil/sec) in replicate tests and a theoretical density of specific gravity of 0.83. Since this material was introduced late in the program, it was not possible to fully characterize and optimize the HMT system. It was possible, however, to obtain small-scale motor test data with the HMT system with only slight modification of the sample configuration in the test motor. These data are presented in the small-scale test motor section.

f. Mechanical Properties and Bond Characterization

A series of formulations were made to evaluate the effect of MNA and DER-332 levels on insulation mechanical properties, using variations of the PBAN mastic binder system used in the four candidate insulation systems which consists of 7.5 equivalents of PBAN terpolymer; 85 equivalents of methyl nadic anhydride (MNA); 7.5 equivalents of poly 1,4-butylene glycol (LD-124); and 110 equivalents of a diglycidyl ether of Bisphenol A (DER-332). Figure 18 shows the results of these tests. Consistent with previous results obtained with this binder system, decreasing the DER-332 resulted in a lower elongation. Increasing the DER-332 content gave a decrease in tensile strength and modulus with an increase in elongation. Reducing the MNA level resulted in

III.C. Discussion of Results (cont.)

lower tensile strengths with some improvement of strain capability. Mechanical properties of a second candidate insulation system (Figure 18), using the basic binder system were similar to those obtained with the first composition. Based on these results the basic binder composition was used for the small-scale motor tests.

Insulation bond test specimens of the candidate materials were prepared with and without SD-886 liner. The bond of SD-886 to propellant and steel was also tested as a control. The data (Figure 19) indicates that the SD-886 liner will be required to insure adequate bond of insulation to propellant. Tests were also run to evaluate the bond of the candidate light-weight (outer layer) system to various chamber materials. Excellent bond strengths were obtained for both titanium and fiber glass chamber materials.

g. Storage Stability of Candidate Insulations

Storage stability tests were conducted with the three experimental candidate insultions IBT-121, IBT-122 and IBT-123. These three materials make up the experimental portion of the four candidate insulation system. Tests were conducted to evaluate the vacuum storage stability of the insulation material and the temperature storage stability of the insulation system in combination with the SD-886 liner and ANB-3405-1 propellant. Because it was introduced late in the program, more limited data was obtained for the IBT-124.

Samples were prepared and stored either in a vacuum container or in an oven, then removed and tested at monthly intervals for a three month period. Insulation specimens were stored in a vacuum of 1.33×10^{-5} N/cm^2 (10^{-5} torr) and tested for weight loss, mechanical properties, thermal conductivity and char rate. Bulk samples of ANB-3405-1

III.C. Discussion of Results (cont.)

cast onto SD-886 lined insulation were stored at 120°F and tested for bond strength.

The effect of storage under high vacuum 1.33×10^{-5} N/cm^2 (10^{-5} torr) conditions at ambient temperature on the mechanical properties of the candidate insulation systems appears to be negligible with the possible exception of the IBT-123. These data are shown in Figure 20. The IBT-123 appears to have hardened but still meets the chamber strain requirement of greater than two percent. No significant changes occurred in ablation rate, thermal conductivity or specific gravity (weight loss) as a result of storage in a space vacuum environment. Figure 21 shows the results of these tests.

Bulk samples of the candidate insulation systems were coated with SD-886 liner to insure a satisfactory bond to the ANB-3405-1 propellant then cast with excess propellant from the batch used to cast the small-scale motor grains. These bond evaluation samples were stored at 120°F and tested monthly for a three month period to assess the effects of elevated temperature storage on the bond. In general, the bond strengths obtained (Figure 22) reflect very little effect of elevated temperature on the insulation-liner-propellant bond system. There was however some difficulty experienced in sample preparation. Since the insulation-liner-propellant specimens were cast as bulk storage specimens, it was necessary to cut smaller test samples from the bulk material. To prepare these samples it was necessary to bond the insulation to one steel plate and the propellant to another steel plate with a secondary adhesive to test tensile or shear strength of the system. In some cases the bond of the propellant to steel plate failed resulting in apparent bond strength values not representative of the same propellant-to-liner bond.

III.C. Discussion of Results (cont)

3. Small-Scale Motor Tests (Task 4)

The four candidate insulation materials selected from the laboratory test results in Task 2 were evaluated in small-scale ballistic test motors in this task. In addition to the four candidate systems, one additional insulation system was evaluated for the reasons explained in the discussion of candidate selection (III.C.2.e). The small-scale ballistic test motor used in this task is illustrated in Figure 23 along with the insulation test segment configurations. Orientation of the insulation segments and measurements of the surface regression rate were made so as to eliminate the differences in ablation rate between top and bottom observed in some end burning motors.

A total of eight small-scale motor tests were made consisting of duplicate tests of each of the four candidate insulation systems and four tests of the add-on HMT formulation. The section containing the test specimens for the first four motors was insulated over one-half of its surface with the candidate material and over the remaining one-half with Gen-Gard V-4030 which served as a control. For the remaining four motor tests a three segmented test specimen was used with one-third segments each of Gen-Gard V-4030 (control), the HMT formulation and one of the candidate systems.

All grains were cast with an 86 wt% solids HTPB propellant formulation from a single 30-gal vertical mixer batch. Nozzles were sized to give an average chamber pressure of 89.6 N/cm^2 (130 psia). Each motor was instrumented for pressure measurement. In addition, Cromel-Alumel jacketed thermocouples with a maximum operating temperature range of 1504°K (2250°F) were installed in the insulation test specimens at 1.5 cm (0.6 inches) and one at 0.76 cm (0.3 inches) from the insulation surface in order to assess the thermal profile in the test material during and after firing. Post-test measurements included thickness loss and char retention characteristics of the materials.

Analysis of the test data was performed to permit scaling from small-scale tests to the full-scale motor. This was accomplished by employing

III.C. Discussion of Results (cont)

the basic thermal model for a charring ablator which uses both the thermophysical properties of materials which decompose (ablate) and the nonablating conduction properties as determined in standard laboratory tests.

a. Propellant Optimization

Three laboratory-scale propellant batches of ANB-3405 were prepared to optimize the propellant formulation for casting the end-burning propellant grains for the small-scale motor (10KS-2500) tests. The propellant mechanical properties data shown in Figure 24 indicated excellent properties were obtained by using 67 equivalents of the TDI curing agent. Viscosity buildup data showed that these unplasticized formulations were very limited in potlife, and reformulation was necessary to improve potlife.

A second series was made, as shown in Figure 25, to obtain a longer potlife. The viscosity buildup data showed that the objective was achieved and the improvement in potlife is evident by comparison with the data for the control propellant batch 10GP-4940. Based on this data the IPDI level selected for the motor batch was 65 equivalents.

A 400-lb batch of ANB-3405-1 propellant was prepared, and eight (8) propellant grains were successfully cast. The basic formulation for this propellant is shown in Figure 22.

b. Small-Scale Motor Tests No. 1 and No. 2

The first two small-scale motors were prepared and fired containing one candidate light-weight insulation and a Gen-Gard V-4030 control. The two candidate light-weight insulations in these initial tests were:

III.C. Discussion of Results (cont)

Motor No. 1 IBT-122
Motor No. 2 IBT-121

Each segment of insulation in the blast tubes (two candidates and two V-4030 controls) contained thermocouples to monitor the combined effects of ablation and heat conduction through the insulation.

Difficulty was experienced with controlling pressure on the firings as evidenced by the pressure-time traces shown in Figure 27. The first motor used a nozzle with an initial throat diameter of 1.158 cm (0.456 inches) which was calculated to provide the design pressure of 89.6 N/cm^2 (130 psi). Deposition of aluminum oxide in the nozzle throat caused an increase in pressure to 289 N/cm^2 (419 psi) and shortened the duration to 100 seconds. The post-fire nozzle diameter was 0.625 N/cm^2 (0.246 inches). On the second motor firing the nozzle throat diameter was increased to 1.615 N/cm^2 (0.636 in.) to compensate for the deposition, and this resulted in a very low initial pressure apparently due to poor ignition. Subsequent throat deposition gave a progressive pressure increase to a maximum of over 207 N/cm^2 (300 psi). Post-fire measurement of the nozzle indicated a nozzle diameter of 1.016 N/cm^2 (0.400 in.).

As indicated by the average ablation rates shown in Figure 28, both candidate insulations appeared to ablate at significantly higher rates than the Gen-Gard V-4030 control. The actual measured rates for the two candidates 0.094 and 0.071 mm/sec (3.7 and 2.8 mils/sec), respectively agree very closely with LITE motor data for these materials, but the control V-4030 showed ablation rates 0.051 and 0.043 mm/sec (2.0 and 1.7 mils/sec) much lower than the LITE motor. This divergence of the ablation measurements was apparently a result of the higher-than-planned operating pressure in the small-scale motors.

Thermocouple data from these first two tests are presented graphically in Figures 29 through 31. No data was obtained from the

III.C. Discussion of Results (cont)

V-4030 thermocouples in the first test because of a malfunction. These data show that the higher ablation rates of the candidate insulations are reflected in higher temperatures seen by the thermocouples. The data in Figure 31 do indicate that a 1.52 cm (0.6 in.) thickness of the ammonium benzoate candidate would limit the case temperature to 366°K (200°F) for a duration of up to 160 seconds.

c. Small-Scale Motor Tests No. 3 and No. 4

The third and fourth small-scale motors were fired with a 10.2 cm (4-in.) I.D. x 15.2 cm (6-in.) long blast tube containing one candidate light-weight insulation and a Gen-Gard V-4030 control. The candidate insulation in these tests were:

Motor #3 - Dual Layer	
(inner layer)	IBT-121
(outer layer)	IBT-123
Motor #4 - Dual Layer	
(inner layer)	Gen-Gard V-4030
(outer layer)	IBT-123

Thermocouples were installed to monitor the temperature profile of the insulation during firing.

Due to the problem of pressure control in the first two small-scale motor firings a new nozzle design was utilized for motors 3 and 4. Carbon nozzles were machined with a throat diameter of 1.615 cm (0.636 in.), the same throat diameter used in the second

III.C. Discussion of Results (cont.)

motor firing. A castable insulation, IBC-111, was then applied to the entrance cone and throat of the carbon nozzle to reduce the throat diameter to 1.270 cm (0.500 in.). This diameter was selected based on a trade off of nozzle deposition rate experienced in the first two firings and the predicted erosion rate of IBC-111. This castable insulation has been used for propellant grain encapsulation and restriction on other Aerojet programs and was selected to provide an evenly eroding throat restrictor which would eliminate aluminum oxide deposition while the IBC-111 remained then allow for some deposition toward the end of the firing.

As evidenced by the pressure-time traces shown in Figure 32, the pressure progressed to over 207 N/cm^2 (300 psia) in each firing, analysis of the data indicates that after the IBC-111 in the throat eroded away, deposition in the throat area was much greater than expected and caused a continuous increase in pressure.

As in motors 1 and 2 the candidate insulation systems in motors 3 and 4, presented in Figure 33, ablated at a higher rate than the Gen-Gard V-4030 control. Candidate insulation ablation rates measured in small-scale motors agree with LITE motor ablation rates and the Gen-Gard V-4030 controls in small-scale motors show ablation rates much lower than in the LITE motors.

Insulation temperature profiles taken at the thermocouples in the small-scale motor are presented in Figures 34 through 37. The higher ablation rates of the candidate insulation are again reflected in the higher temperatures recorded for these systems.

III.C. Discussion of Results (cont.)

To quantitatively assess the effect of the higher pressures experienced in the first four small-scale motor firings, a series of LITE motor tests were conducted over the pressure range experienced in motor tests with the candidate insulation systems and the Gen-Gard V-4030. LITE motor tests results, shown in Figure 38, indicate a rather drastic effect of increased pressure on ablation rate of the candidate insulations. This rather large difference in ablation rate between the two candidate insulation systems, IBT-121, IBT-122 and Gen-Gard V-4030 at higher chamber pressures explains the apparent differences observed in the performance of these systems in the small-scale motor tests which operated at higher pressures.

d. Small-Scale Motor Tests No. 5 and No. 6

Nozzles for motors No. 5 and No. 6 were redesigned to include an ablative throat material to compensate for the severe deposition experienced in the previous four motor firings. The nozzle for Motor No. 5 contained a silica-phenolic insert in a nozzle material of IBC-111. The nozzle for motor No.6 contained a castable carbon insert in a nozzle material of IBC-111.

Pressure-time curves for the two motor firings shown in Figure 39 indicate the desired operating pressure was not achieved. Observation of the fired nozzle used in Motor No. 5 showed severe erosion of the IBC-111 and silica-phenolic insert which resulted in the erratic behavior of the pressure-time trace. Analysis of the fired nozzle and pressure-time trace for Motor No. 6 shows the nozzle insert material (castable carbon) was ejected on ignition (possibly cracked) resulting in a malfunction of the motor. No usable data were obtained from the sixth motor firing.

III.C. Discussion of Results (cont.)

The insulation test configuration used in the fifth motor firing was changed from the two-segmented tube to a three-segmented tube to accommodate the test evaluation of a second insulation system. Insulation systems evaluated in the fifth motor were:

(1) IBT-121
(2) IBT-124
(3) Gen-Gard V-4030 (control)

Ablative performance for these insulation systems is summarized in Figure 40. Again the ammonium benzoate formulation performed similarly to the LITE motor tests. Of particular note, however, is the ablative performance of the formulation containing hexamethylene tetramine (HMT). The performance of the HMT formulation in the operating conditions of Motor No. 5 was somewhat better than the Gen-Gard V-4030. Thermocouple traces for this motor firing (Figure 41) indicate the 1.52 cm (0.6-in.) thickness insulation was completely satisfactory case protection.

e. Small-Scale Motor Tests No. 7 and No. 8

Nozzles for Motors No. 7 and No. 8 were again redesigned to eliminate the problems experienced with the previous motor firings. These nozzles consisted of a sandwiched ablative insert of asbestos-phenolic and fibrous graphite potted into a carbon exit cone with IBC-111. The nozzle design is illustrated in Figure 42. Pressure-time curves (Figure 43) for the seventh and eighth tests indicate the ablative material did not compensate for nozzle deposition. Again, as in the first set of motor tests, the motors operated at a significantly higher pressure than the 89.6 N/cm^2 (130 psia) design pressure.

Insulation systems tested in the seventh and eighth motor firings were:

III.C. Discussion of Results (cont.)

Motor #7 - Dual Layer

(1) (inner layer) Gen-Gard V-4030
(outer layer) IBT-123

(2) (inner layer) IBT-124
(outer layer) IBT-123

(3) Gen-Gard V-4030 (control)

Motor #8

(1) IBT-122

(2) IBT-124

(3) Gen-Gard V-4030 (control)

Performance data for these insulation systems are summarized in Figure 44. In each case the insulation system using HMT showed excellent performance compared to the Gen-Gard V-4030. Similar results to the initial motor firing were obtained with the $(NH_4)_2SO_4$ formulation.

Temperature profile data for the last two motor firings in the series are shown in Figures 45 and 46. In each case the insulation system using the HMT filler material performed as well or better than the Gen-Gard V-4030 control.

f. Analysis of Candidate System Performance

It was clear from the small-scale motor test data that the IBT-124 system using the HMT/$(NH_4)_2SO_4$ filler combination was far superior to any of the other candidate insulations and the only one which exhibited a significant improvement in performance compared to V-4030. Therefore a detailed analysis was performed to quantitatively assess the capabilities of this insulation in a typical planetary orbitor motor, relative to the control (V-4030).

III.C. Discussion of Results (cont.)

The data available for analysis of the insulation performance consists of thermal property tests measured in the laboratory and subscale motor test data including insulation ablation rates and thermocouple data from thermocouples embedded in the candidate insulation materials.

The subscale motors were instrumented at depths of approximately 0.76 and 1.53 cm (0.3 and 0.6 inches) from the original surface. The intent was to collect test data which could be matched by a thermal model using the thermal properties based on laboratory test data. Placement of the thermocouples could not be accomplished with sufficient accuracy to make the desired correlation. Some conclusions can however be drawn from the subscale data. Typical test data is shown in Figure 47 comparing Gen-Gard V-4030 and the IBT-124 and IBT-124/IBT-123 composite. These data indicate that under like conditions the two insulation systems exhibit ablation rates equal to or less than Gen-Gard V-4030. The thermocouple data although subject to problems mentioned above can be analyzed by assuming the same errors in location occurred in both materials. Comparable data on both materials exists at the 1.52 cm (0.6 inch) depth. These data in Figure 47 indicate that the IBT-124 and IBT-124/IBT-123 temperature rises were less than those for Gen-Gard V-4030.

A thermal model was constructed using the thermal properties for IBT-124 and IBT-123 measured in lab tests. These properties are shown in Figure 48. The thermal model was used to analyze a typical Jupiter Orbiter Duty Cycle, compared with the V-4030 analysis for the same environment. The duty cycle assumed was a 200-second action time and average pressure of 89.6 N/cm^2 (130 psi).

III.C. Discussion of Results (cont.)

The results are shown in Figure 49 which illustrates the ablation rates are essentially the same and also the temperature gradients are similar. The approach employed in sizing thicknesses of each material is based on the assumption that sufficient IBT-124 material is used to accommodate the ablation and the allowable case temperature is maintained by varying the IBT-123 substrata.

The thermal analysis and limited subscale test data indicates that comparable thermal protection can be achieved with the IBT-124/IBT-123 composite on an actual thickness basis. Based on this analysis, the minimum improvement in weight performance that can be expected with the IBT-124/IBT-123 dual layer composite is 1.6:

	Insulation System	Thickness	Sp. Gr.	Product (T x sp.gr.)
Dual Layer	IBT-124	0.3	.83	.248
	IBT-123	0.3	.55	.165
				.413
	V-4030	0.6	1.1	.66

$$\text{Improvement} = \frac{.66}{.413} = 1.6$$

Since the program goal was to achieve an insulation weight performance twice that of Gen-Gard V-4030 or a 50% savings in weight the IBT-124 material appears to have achieved better than 60% of that goal.

4. Development of Insulation Fabrication Methods Task 3

This task was designed to develop and demonstrate a suitable installation technique for the primary lightweight insulation

III.C. Discussion of Results (cont.)

systems selected from the results of the small-scale motor tests. Preliminary development work was conducted in conjunction with the small-scale motor tests. The chamber selected for the final demonstration was a surplus satellite retromotor designated SVM-2. This chamber is similar in configuration to the full-scale space application motor which would utilize the candidate insulation. The chamber dimensions are 50.8 cm (20-inches) long and 55.9 cm (22-inches) in diameter with a cylindrical section 5-inches from equator to equator.

Thickness control guides were found to be the most successful means of accurately controling the thickness of the five insulation systems tested in the small-scale motor task. For the SVM-2 chamber demonstration thickness control guides were fabricated to yield an insulation profile similar to the NASA JPL SR-28-4 motor insulation configuration 2. The insulation thickness in the aft dome section of the chamber is 1.52 cm (0.6-inches) and has a smooth taper from 1.52 cm (0.6-inches) to 0.58 cm (0.2-inches) at the equator of the fore dome section. From the equator of the fore dome section to the apex the insulation thickness is constant at 0.58 cm (0.2-inches).

Two insulations were selected for installation in the SVM-2 chamber. Both systems are representative of all the candidate insulations evaluated in the small-scale motor task. The final insulation used was IBT-122, a PBAN mastic containing 35 wt% $(NH_4)_2SO_4$, 10 wt% Kaowool fiber and 15 wt% FTD-202. Thickness control guide strips were installed to cover approximately one eighth of the chamber from fore-to-aft. Two batches of insulation were prepared and using a Hobart mixer troweled in place between the guide strips. During the troweling operation care was exercised

III.C. Discussion of Results (cont.)

to avoid air entrapment. The final leveling operation was accomplished with a contoured metal trowel placed across the thickness control guide strips. The photographs in Figures 50 and 51 show the installed segment of insulation with guide strip in place. The second insulation was IBT-124, a PBAN mastic containing 17.5 wt% HMT, 17.5 wt% $(NH_4)_2SO_4$, 10 wt% Kaowool and 15 wt% FTD-202. This insulation was installed in a similar manner as the first insulation system.

After completion of the cure cycle for the two insulations, they were removed and sectioned for measurements and fluoroscope examination. Fluoroscopic examination of representative sections showed no large internal voids. One shallow void was found at the chamber to insulation interface in an area of the chamber that was not visible during the installation operation. Access to this area through the relatively small opening in the chamber was particularly difficult.

The insulation thickness profile for IBT-124 is shown in Figure 52. Indications are that to achieve close tolerances of a thickness profile, such as in the SVM-2 chamber, it would be necessary to machine the final dimension. This technique has been used for a similar insulation (IBC-118) during another program. It is quite probable, however, with repeat practice, larger access area and additional guide strips placed somewhat closer together much improved thickness control would be achieved with these trowelable insulations.

IV. CONCLUSIONS

An advanced light-weight insulation system was developed for use in space motor applications which exhibits the potential for significant weight performance gain compared to the control V-4030. The insulation system consists of a dual layer composite of IBT-124 and IBT-123 insulating materials. The IBT-123 substrate material is characterized by very low specific gravity, very low thermal conductivity and moderate ablation properties while the IBT-124 primary insulation is characterized by low specific gravity, moderate thermal conductivity and low ablation rate.

Performance of the improved insulation was compared to the performance of Gen-Gard V-4030, a commercially available EPDM rubber currently in use in space motor applications. The weight performance of the improved insulation system was found to be a minimum of 1.6 times that of the EPDM rubber.

The improved performance of the insulation system was achieved through the use of very low density microballoons with high performance fibrous and particulate fillers for the low ablation rate insulation (IBT-124). Microballoons were used exclusively for the filler of the IBT-123 very light weight material.

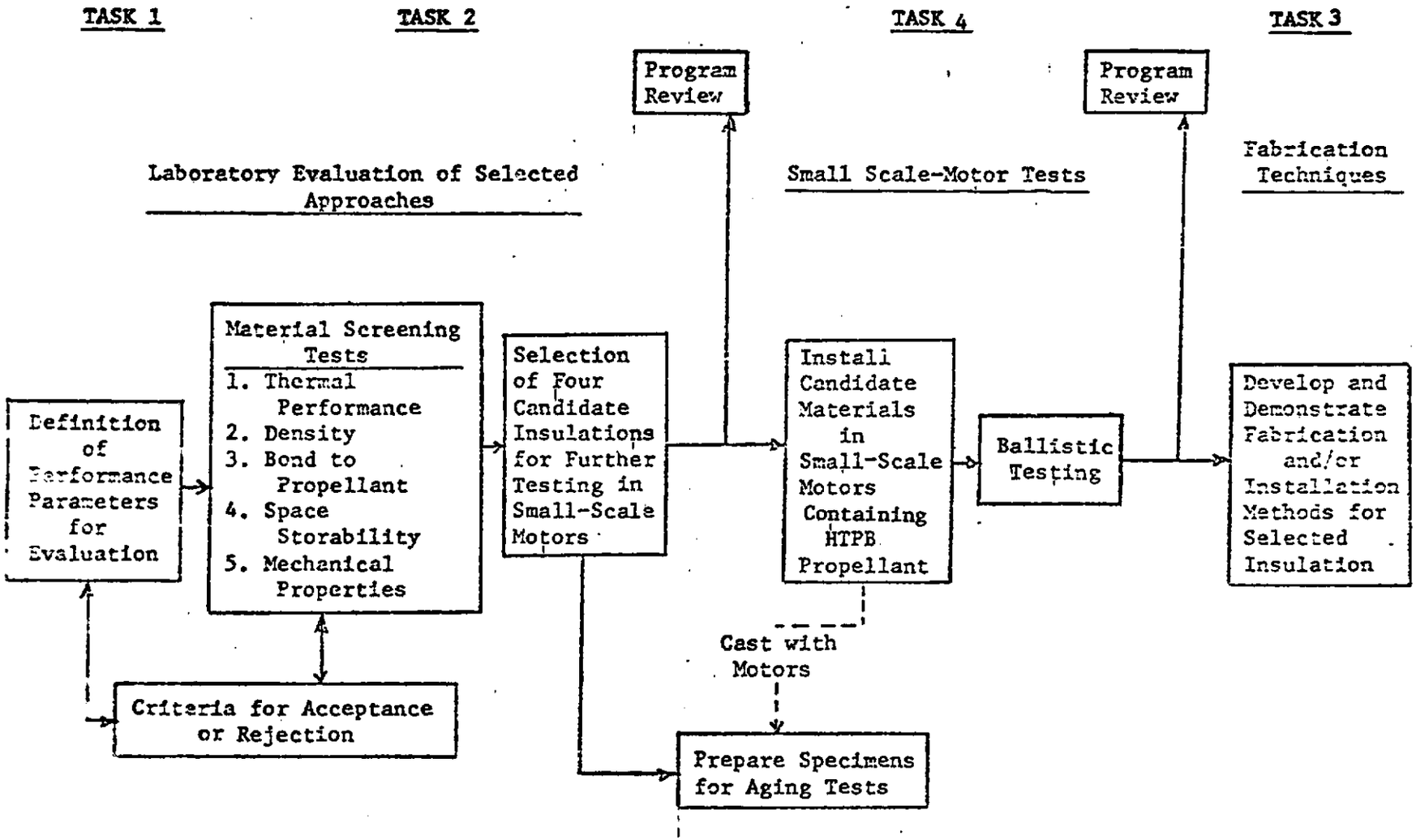

PROGRAM PLAN FOR DEVELOPMENT OF ADVANCED LIGHTWEIGHT INSULATION

Critical Performance Parameter	Performance Criteria: Continue Evaluation	Performance Criteria: Continue Only if Warranted by Overall Performance Potential	Performance Criteria: Terminate Evaluation
I. THERMAL PERFORMANCE			
A. SINGLE LAYER			
1. Thermal Conductivity, J/cm-sec-°F (BTU/hr-ft-°F)	<0.08	0.08-0.12	>0.12
2. Char Rate, mm/sec (mils/sec)	<0.038 (<1.5)	0.038-0.076 (1.5-3.0)	>0.076 (>3.0)
3. Specific Gravity	<0.55	0.55-0.90	>0.90
4. Weight Performance Potential	>2.0 x Gen-Gard V-4030	>1.8 x Gen-Gard V-4030	<1.8 x Gen-Gard V-4030
B. DUAL LAYER			
1. Top or Low-Char-Rate Layer			
a. Thermal Conductivity, J/cm-sec-°K (BTU/hr-ft-°F)	<0.15	0.15-0.20	>0.20
b. Char Rate, mm/sec (mils/sec)	<0.025 (<1.0)	0.025-0.064 (1.0-2.5)	>0.064 (>2.5)
c. Specific Gravity	<1.0	1.0-1.3	>1.3
2. Bottom or Low-Thermal-Conductivity Layer			
a. Thermal Conductivity, J/cm-sec-°K (BTU/hr-ft-°F)	<0.04	0.04-0.08	>0.08
b. Specific Gravity	<0.40	0.40-0.70	>0.70
3. Weight Performance Potential	>2.0 x Gen-Gard V-4030	>1.8 x Gen-Gard V-4030	<1.8 x Gen-Gard V-4030
II. BONDING TO PROPELLANT AND CASE			
A. INITIAL BOND STRENGTH TO PROPELLANT 298°K (77°F)			
1. Tensile and Shear Strength, N/cm^2 (psi)	Propellant Cohesive Strength	>60% of Propellant Cohesive Strength	<60% of Propellant Cohesive Strength
B. BOND STORAGE STABILITY AT 322°K (120°F)	No significant Change	10-30% Decrease	>30% Decrease
C. INITIAL BOND STRENGTH TO CASE MATERIALS [(TENSILE, N/cm^2 (psi)]	>1.38 (200)	69-138 (100-200)	<69 (100)

Report CR 114513

Figure 2
Page 1 of 2

Advanced Lightweight Insulation Development,
Critical Performance Parameters and Criteria

ADVANCED LIGHTWEIGHT INSULATION DEVELOPMENT (cont)

Critical Performance Parameter	Performance Criteria: Continue Evaluation	Performance Criteria: Continue Only if Warranted by Other Outstanding Properties	Performance Criteria: Terminate Evaluation
III. MECHANICAL PROPERTIES			
A. BIAXIAL STRAIN CAPABILITY (HIGH RATE)	>5%	2-5%	<2%
B. THERMAL CYCLING STRAIN CAPABILITY	>5%	2-5%	<2%
IV. SPACE STORABILITY (3 MONTHS AT 10^{-5} TORR)			
A. MECHANICAL PROPERTIES	No Significant Change	± 10-30% Change	>30% Change
B. DENSITY	No Significant Change	<1% Change	>1% Change
C. THERMAL CONDUCTIVITY	No Significant Change	<1% Change	>1% Change
D. CHAR RATE	No Significant Change	10% Increase	10% Increase

Advanced Lightweight Insulation Development,
Critical Performance Parameters and Criteria

FLOW DIAGRAM OF WORK PERFORMED UNDER TASK 2
LABORATORY TESTING EFFORT

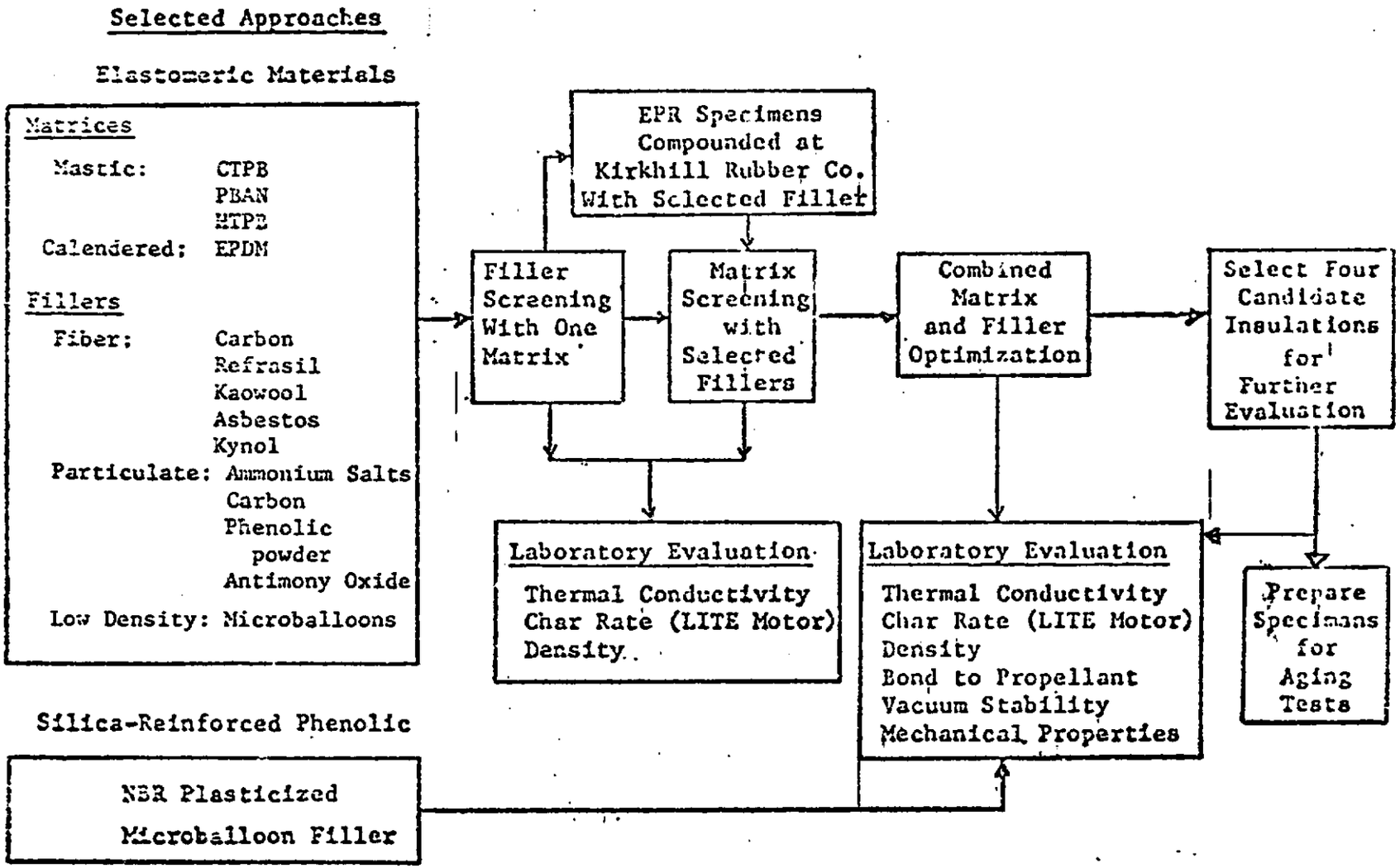

Figure 3

Flow Diagram of Work Performed Under Task 2 Laboratory Testing Effort

Lab. Insulation Test Evaluator

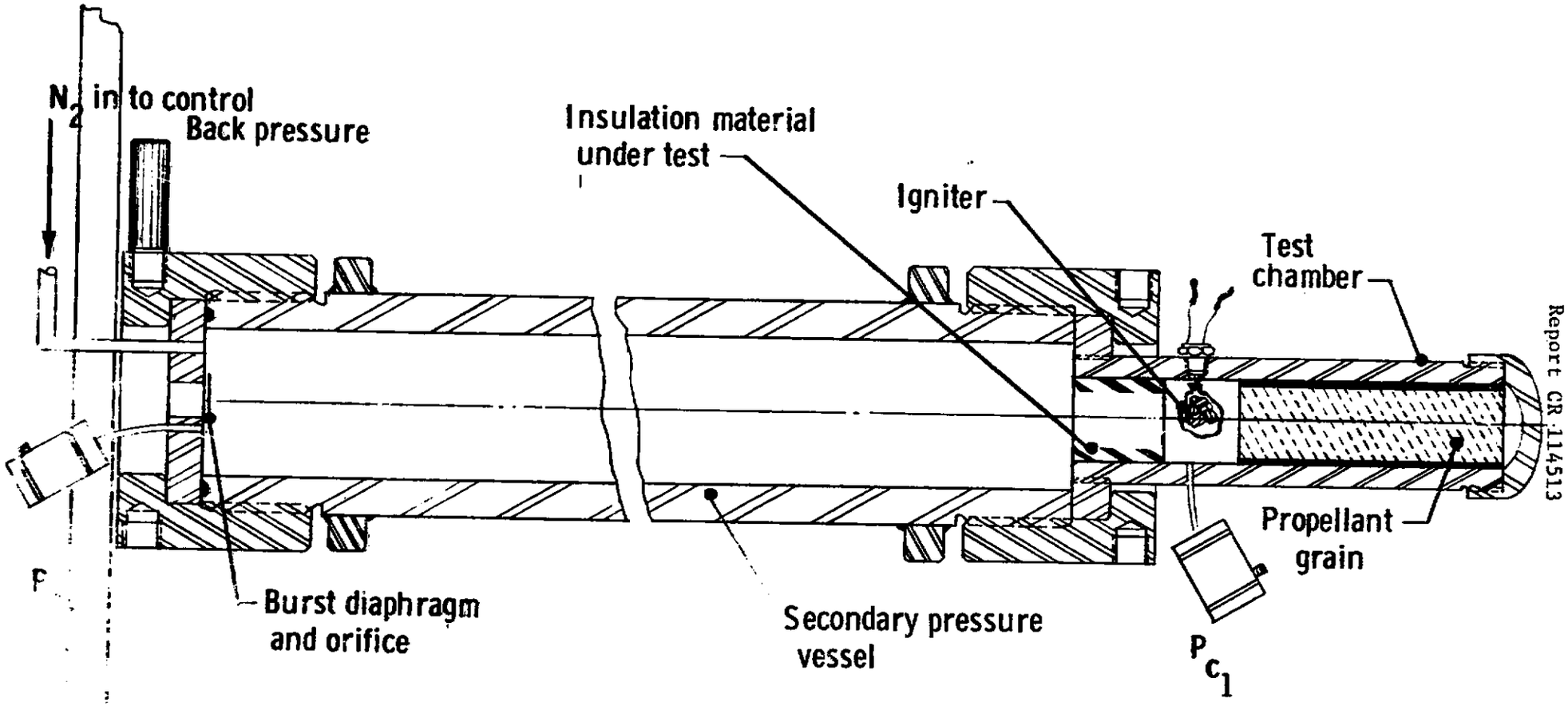

Report CR-114513

Figure 4

LITE Motor

Insulation	LITE Motor Operating Conditions							Specific Gravity
	Duration, Second	Pressure, N/cm^2	(psia)	Propellant Burn Rate cm/sec	(in./sec)	Insulation Ablation Rate, mm/sec	(mils/sec)	
GenGard V-4030	19.61	89.6	(130)	0.46	(0.18)	0.081	(3.2)	1.10
	18.07	100	(145)	0.48	(0.19)	0.081	(3.2)	
	19.50	89.6	(130)	0.46	(0.18)	0.069	(2.7	
USR-3804	20.67	89.6	(130)	0.43	(0.17)	0.071	(2.8)	1.12
GenGard V-44	18.07	100	(145)	0.56	(0.22)	0.084	(3.3)	1.27

Figure 5

LIT Motor Ablation Measurements of Commercially Available Insulations

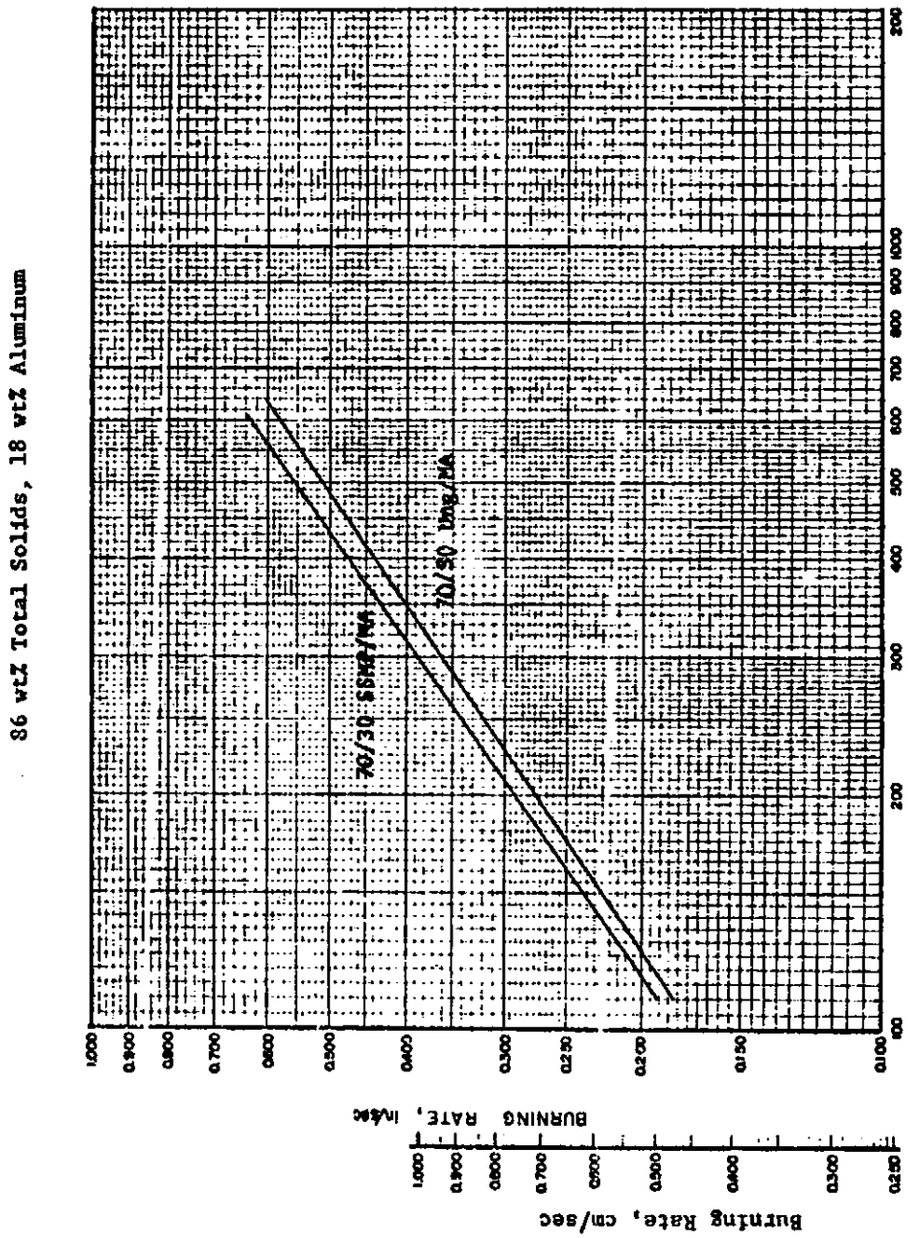

Solid Strand Burning Rates of ANB-3405 Propellant

Figure 6

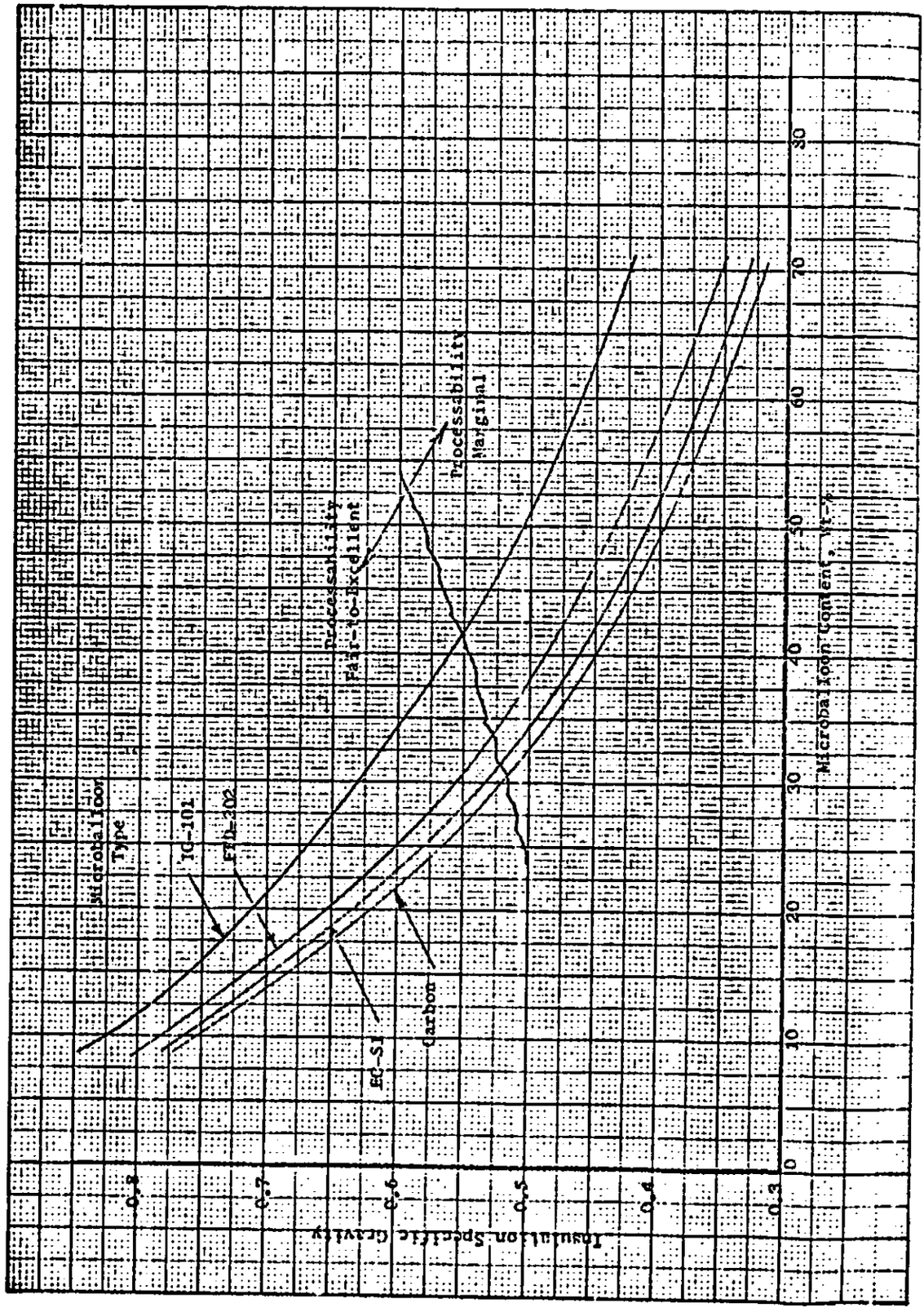

Effect of Microballoon Content on Insulation Specific Gravity and Processability (CTPB Mastic)

Figure 7

EFFECT OF MICROBALLOON TYPE AND CONTENT ON ABLATION RATE OF CTPB MASTIC INSULATION

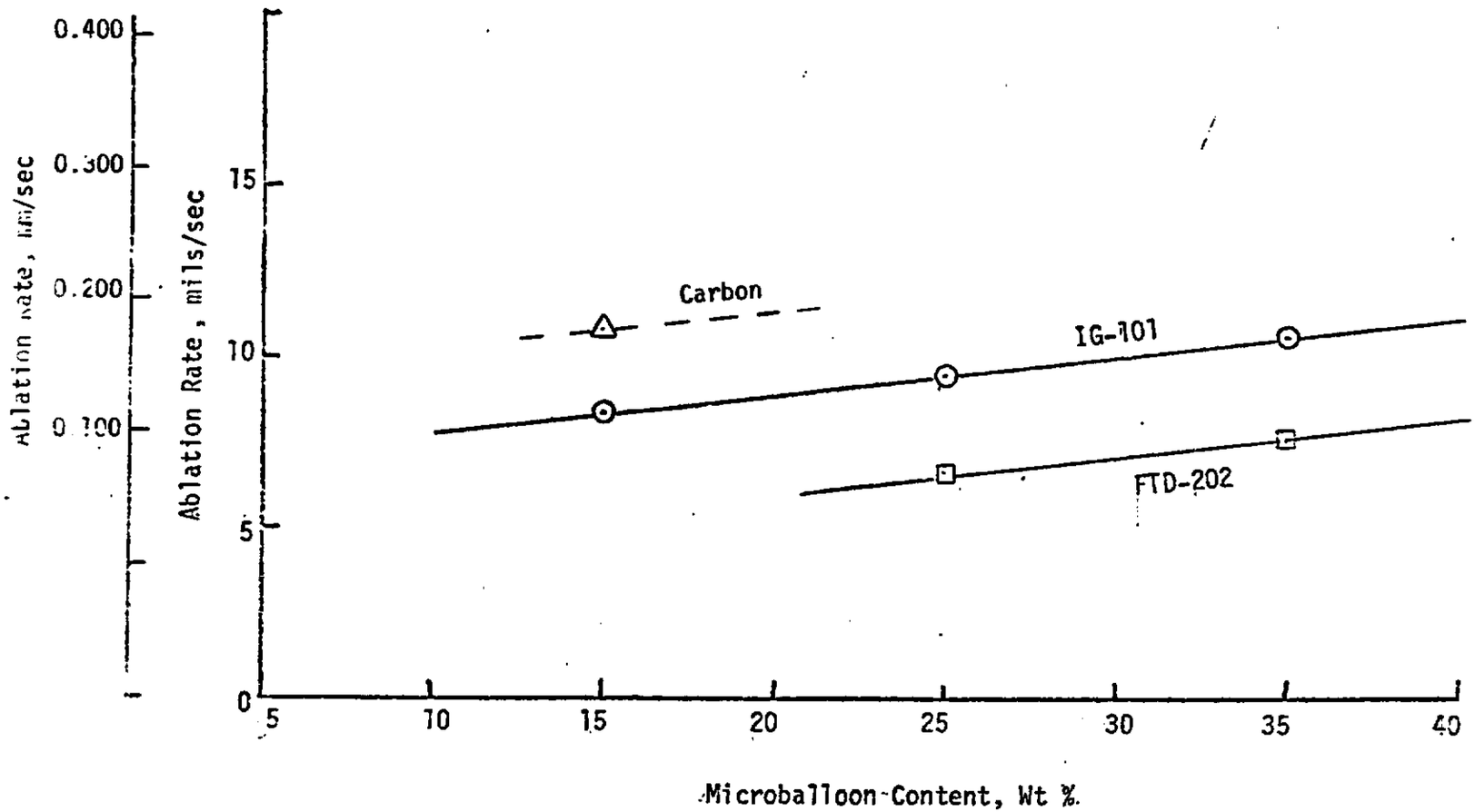

Figure 8

Effect of Microballoon Type and Content on Ablation Rate of CTPB Mastic Insulation

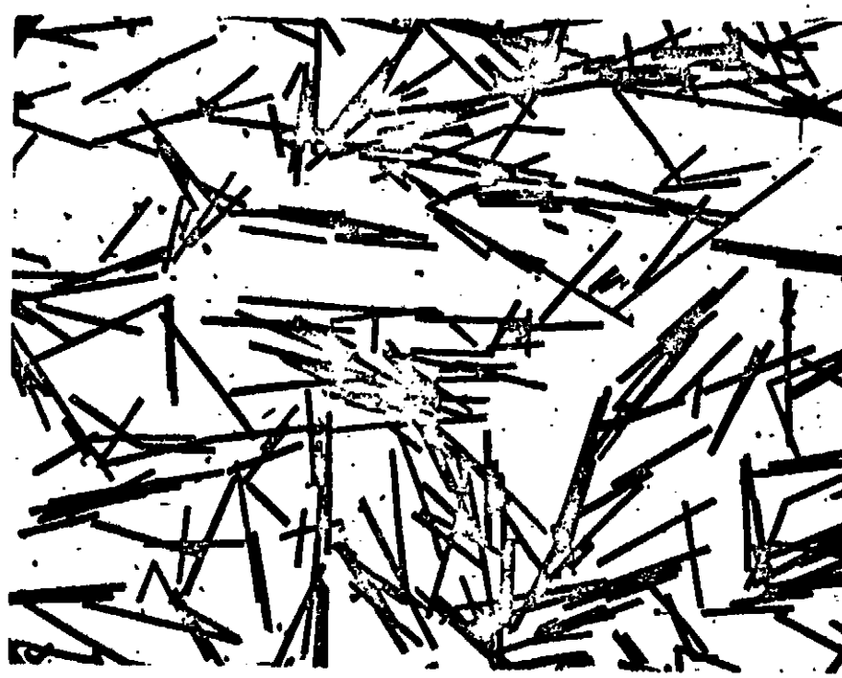

PHOTOMICROGRAPH (40X) OF GROUND CARBON FIBERS

Figure 9

Insulation	LITE Motor Operating Conditions					Insulation Ablation Rate,		Specific Gravity
	Duration, Second	Pressure, N/cm2	(psia)	Propellant Burn Rate cm/sec	(in./sec)	mm/sec	(mils/sec)	
CTPB Mastic with 30 wt% Carbon Fiber	19.04	89.6	(130)	0.46	(0.18)	0.130	(5.1)	1.12
CTPB Mastic with 30 wt% Refrasil	18.48	89.6	(130)	0.48	(0.19)	0.119	(4.7)	1.20
CTPB Mastic with 30 wt% Kaowool	16.70	96.5	(140)	0.53	(0.21)	0.119	(4.7)	1.26
PBAN Mastic with 30 wt% Kaowool	20.93	89.6	(130)	0.43	(0.17)	0.117	(4.6)	1.26
PBAN Mastic with 30 wt% Asbestos	19.15	89.6	(130)	0.46	(0.18)	0.079	(3.1)	1.30
PBAN Mastic 10 wt% Asbestos	19.15	89.6	(130)	0.46	(0.18)	0.084	(3.3)	1.14
PBAN Mastic 30 wt% Kynol	20.46	100	(145)	0.43	(0.17)	0.094	(3.7)	1.11

Figure 10

LIT Motor Ablation Measurements of Advanced Lightweight Insulations

Insulation	LITE Motor Operating Conditions: Duration, Second	Propellant Burn Rate*: cm/sec	Propellant Burn Rate*: (in./sec)	Insulation Ablation Rate, mm/sec	Insulation Ablation Rate, (mils/sec)	Specific Gravity
CTPB Mastic with 25 wt% $(NH_4)_2SO_4$	18.85	0.48	(0.19)	0.084	(3.3)	1.05
CTPB Mastic with 50 wt% $(NH_4)_2SO_4$	19.60	0.46	(0.18)	0.071	(2.8)	1.25
CTPB Mastic with 75 wt% $(NH_4)_2SO_4$	18.82	0.48	(0.19)	0.064	(2.5)	1.47
CTPB Mastic with 30 wt% ground Micarta	20.73	0.43	(0.17)	0.091	(3.6)	1.06

*Chamber operating pressure 89.6 N/cm^2 (130 psia)

Figure 11

LITE Motor Ablation Measurements of Advanced Lightweight Insulations

Insulation	LITE Motor Operating Conditions: Duration, Second	Propellant Burn Rate*: cm/sec	Propellant Burn Rate*: (in./sec)	Insulation Ablation Rate, mm/sec	Insulation Ablation Rate, (mils/sec)	Specific Gravity
CTPB Mastic with 30% $(NH_4)_2SO_4$ 30% Kaowool	21.88	0.41	(0.16)	0.081	(3.2)	1.48
CTPB Mastic with 30% $(NH_4)_2SO_4$ 30% FTD-202	20.69	0.43	(0.17)	0.114	(4.5)	0.61
CTPB Mastic with 30% $(NH_4)_2SO_4$ 10% Kaowool 10% FTD-202	18.87	0.48	(0.19)	0.086	(3.4)	0.93
CTPB Mastic with 30% $(NH_4)_2SO_4$ 10% Kaowool 20% FTD-202	18.79	0.48	(0.19)	0.081	(3.2)	0.75
CTPB Mastic with 35% $(NH_4)_2SO_4$ 10% Kaowool 15% FTD-202	18.56	0.48	(0.19)	0.081	(3.2)	0.85
CTPB Mastic with 20% $(NH_4)_2SO_4$ 20% Kaowool 20% FTD-202	18.00	0.51	(0.20)	0.124	(<4.9**)	0.77

* Chamber operating pressure 89.6 N/cm^2 (130 psia)
** Virgin insulation removed with char layer.

Figure 12

LITE Motor Ablation Measurements of Advanced Lightweight Insulations

Insulation	LITE Motor Operating Conditions: Duration, Second	Propellant Burn Rate* cm/sec	Propellant Burn Rate* (in./sec)	Insulation Ablation Rate, mm/sec	Insulation Ablation Rate, (mils/sec)	Specific Gravity
CTPB Mastic with 10% Kaowool 35% $(NH_4)_2SO_4$ 15% FTD-202	18.56	0.48	(0.19)	0.081	(3.2)	0.85
PBAN Mastic with 10% Kaowool 35% $NH_4C_7H_5O_2$ 15% FTD-202	19.45	0.46	(0.18)	0.066	(2.6)	0.81
PBAN Mastic with 10% Asbestos 35% $(NH_4)_2SO_4$ 15% FTD-202	17.70	0.51	(0.20)	0.099	(3.9)	0.87
PBAN Mastic with 10% Asbestos 35% $NH_4C_7H_5O_2$ 15% FTD-202	20.02	0.46	(0.18)	0.028	(1.1)	0.81
PBAN Mastic with 10% Kynol 35% $(NH_4)_2SO_4$ 15% FTD-202	20.11	0.46	(0.18)	0.099	(3.9)	0.84

*Chamber operating pressure 89.6 N/cm^2 (130 psi)

Figure 13

LITE Motor Ablation Measurements of Advanced Lightweight Insulations

PBAN Mastic Insulation*	LITE Motor Operating Conditions: Duration, Second	Propellant Burn Rate*: cm/sec	Propellant Burn Rate*: (in./sec)	Insulation Ablation Rate, mm/sec	Insulation Ablation Rate, (mils/sec)	Specific Gravity
35% $(NH_4)_2SO_4$ Ammonium Sulfate	18.44	0.48	(0.19)	0.091	(3.6)	0.87
35% $NH_4C_7H_5O_2$ Ammonium Benzoate	20.02	0.46	(0.18)	0.028	(1.1)	0.81
	22.35	0.41	(0.16)	0.053	(2.1)	
35% $(NH_4)_2HC_6H_5O_7$ Ammonium Citrate	18.45	0.48	(0.19)	0.076	(3.0)	0.84
35% $NH_4H_2PO_4$ Ammonium Phosphate (monobasic)	20.50	0.43	(0.17)	>0.069	(>2.7)	0.87
35% $(NH_4)_2HPO_4$ Ammonium Phosphate (dibasic)	18.71	0.48	(0.19)	0.084	(3.3)	0.86

* All contain: 10% Asbestos Fiber
15% FTD-202 Microballoons

* Chamber operating pressure 89.6 N/cm^2 (130 psia).

Figure 14

LITE Motor Ablation Measurements of Advanced Lightweight Insulations

Insulation Matrix*		LITE Motor Operating Conditions: Duration, Second	Propellant Burn Rate*: cm/sec	Propellant Burn Rate*: (in./sec)	Insulation Ablation Rate, mm/sec	Insulation Ablation Rate, (mils/sec)	Specific Gravity
CTPB Mastic		18,56	0.48	(0.19)	0.081	(3.2)	0.85
		15.60	0.58	(0.23)	0.112	(4.4)	
PBAN Mastic		18.44	0.48	(0.19)	0.091	(3.6)	0.85
		19.04	0.46	(0.18)	0.102	(4.0)	
HTPB Mastic (TDI)Cure)		19.78	0.46	(0.18)	0.122	(4.8)	0.84
HTPB Mastic (DDI Cure)		15.72	0.56	(0.22)	0.193	(7.6)	0.84
Sat. HTPB Mastic (TDI Cure)		17.66	0.51	(0.20)	0.152	(6.0)	0.83
Sat. HTPB Mastic (DDI Cure)		18.87	0.48	(0.19)	0.079	(3.1)	0.80
		19.59	0.46	(0.18)	0.135	(5.3)	
EPDM (Calendered) 20 wt% IG-101	Uncured	19.60	0.48	(0.19)	0.091	(3.6)	0.85
	Cured	16.54	0.53	(0.21)	0.091	(3.6)	0.97

* All mastic systems contained 35 wt % $(NH_4)_2SO_4$.
10 wt % Kaowool
15 wt % FTD-202

** Chamber operating condition 89.6 N/cm^2 (130 psi).

Figure 15

LITE Motor Ablation Measurements of Advanced Lightweight Insulations

Specimen Configuration				Direction of Applied Stress	Test Conditions			Biaxial Mechanical Properties				
No. of Plies	Fabric Orientation in Each Ply	Total Thickness, mm	(in.)		Temperature, °K	(°F)	Strain Rate, min^{-1}	σ_{m_2} N/cm^2	σ_m (psi)	ϵ_b %	E_o N/cm^2	E_o (psi)
3	Weaves parallel in all plies	1.90	(0.075)	Parallel to weave	298	(77)	0.02	1493	(2165)	9.5	43,680	(63,350)
3	Weaves parallel in all plies	1.90	(0.075)	Parallel to fill	298	(77)	0.02	1872	(2715)	1.1	168,500	(244,400)
3	Weaves parallel in all plies	1.90	(0.075)	45° bias to weave	298	(77)	0.02	2034	(2950)	8.1	50,220	(72,840)
6	Weaves oriented 90° with respect to each other in alternate plies	3.81	(0.15)	45° bias to weave	255	(0)	0.02	2955	(4286)	3.7	77,220	(112,000)
6	Weaves oriented 90° with respect to each other in alternate plies	3.81	(0.15)	45° bias to weave	255	(0)	20.0	4298	(6233)	2.4	275,790	(400,000)

NOTE: Specimens cured under 10.3 N/cm^2 (15 psia) pressure at 450°K (350°F) for 3.5 hours.

Figure 16

Mechanical Properties of WB-6320 Phenolic-Impregnated Silica Fabric Insulation

Insulation Identification	Binder	Filler Composition, wt%	Thermal Conductivity J/cm-sec-°K	(BTU/ft-hr-°F)	Specific Gravity	Typical Ablation Rate mm/sec	(mils/sec)
IBT-122	PBAN	35 $(NH_4)_2SO_4$ 10 Kaowool 15 FTD-202	0.104	(0.10)	0.85	0.084	(3.3)
IBT-121	PBAN	35 $NH_4C_7H_5O_2$ 10 Asbestos 15 FTD-202	0.104	(0.10)	0.81	0.051	(2.0)
IBT-123/ IBT-121	PBAN/PBAN (Dual layer)	35 IG-101 (outer layer) 35 $NH_4C_7H_5O_2$ (inner layer) 10 Asbestos 15 FTD-202	0.073 0.104	(0.07) (0.10)	0.60 0.81	0.216 0.051	(8.5) (2.0)
IBT-123 / V-4030	PBAN/EPDM (Dual layer)	35 IG-101 (outer layer) Gen-Gard V-4030 (inner layer)	0.073 0.114	(0.07) (0.11)	0.60 1.1	0.216 0.076	(8.5) (3.0)
	V-4030	(Control)	0.114	(0.11	1.1	0.076	(3.0)

Figure 17

Candidate Insulation Systems

Binder Composition, eq.				Filler Composition, Wt%			Mechanical Properties at 77°F					
PBAN	MNA	LD-124	DER-332	Fiber	Particulate	Microballoon	σ_m N/cm^2	σ_m (psi)	ε_m %	ε_b %	E_o N/cm^2	E_o (psi)
7.5	85	7.5	85	(10) Kaowool	(35) $(NH_4)_2SO_4$	(15) FTD-202	250	(363)	9	11	5196	(7536)
7.5	85	7.5	110	"	"	"	145	(211)	16	21	1895	(2748)
7.5	85	7.5	135	"	"	"	79	(115)	20	35	732	(1061)
23	70	7	85	"	"	"	74	(108)	12	15	879	(1275)
30	63	7	85	"	"	"	63	(92)	15	20	617	(895)
37	56	7	85	"	"	"	54	(79)	14	17	550	(798)
7.5	85	7.5	110	(10) Asbestos	(35) $NH_4C_7H_5O_2$	"	150	(217)	18	49	2195	(3183)

Figure 18

Mechanical Properties of Candidate ASPMI Insulation

Test System	Tensile Strength N/cm^2	(psi)	Break Type
Steel/SD-886/ANB-3405	68	(98)	70 CP/30 CPI
Steel/IBT-121/ANB-3405	17	(23)	API
Steel/IBT-121/SD-886/ANB-3405	52	(75)	CL
Steel/IBT-122/ANB-3405	71	(101)	CP
Steel/IBT-122/SD-886/ANB-3405	35	(50)	ALI
Steel/IBT-123/SD-886/ANB-3405	73	(107)	CP
Titanium/IBT-123	248	(359)	CI
Fiberglass/IBT-123	111	(161)	CF

IBT-121 = PBAN mastic with 35% $NH_4C_7H_5O_2$, 10% asbestos, and 15% FTD-202 microballoons.

IBT-122 = PBAN mastic with 35% $(NH_4)_2SO_4$, 10% Kaowool, and 15% FTD-202 microballoons.

IBT-123 = PBAN mastics with 35% IG-101 microballoons.

Break Type:

CP	Cohesive propellant
CL	Cohesive liner
CI	Cohesive insulation
CF	Cohesive fiberglass
CPI	Cohesive propellant at interface
API	Adhesive propellant-liner
ALI	Adhesive liner-insulation

Candidate Insulation Bonding Characteristics

Figure 19

Mechanical Properties at 298°K

Insulation System	Aging Period, Months	Tensile Strength, σ_m, N/cm^4 (psi)		Elongation, ϵ_b, %	Modulus E_o, N/cm^2 (psi)	
IBT-121	0	198	(287)	4	6272	(9097)
	1	232	(337)	4	6681	(9690)
	2	146	(212)	6	4639	(6728)
	3	205	(298)	4	6519	(9454)
IBT-122	0	132	(191)	21	2236	(3243)
	1	187	(271)	16	4404	(6387)
	2	148	(215)	17	2933	(4254)
	3	195	(283)	15	4131	(5991)
IBT-123	0	139	(201)	11	3376	(4897)
	1	304	(441)	7	9029	(13095)
	2	396	(574)	5	13423	(19469)
	3	459	(666)	4	16721	(24251)
IBT-124	0	224	(325)	10	8527	(12367)
	1.5	273	(396)	9	7148	(10367)
V-4030	0	256	(371)	623	917	(1330)
	1.5	255	(370)	638	803	(1165)

Note: Vacuum level was 1.33×10^{-5} N/cm^2 (10^{-5} torr)

Figure 20

High Vacuum Storage Stability Evaluation of Candidate Advanced Insulations

LITE Motor and Thermal Conductivity

Insulation System	Aging Period, Months	Insulation Ablation Rate, mm/sec	(mils/sec)	Conductivity (BTU/ft-hr-°F) J/cm-sec-°F		Weight Loss, %
IBT-121	0	0.071	(2.8)	0.097	(0.093)	--
	1	0.094	(3.7)	0.109	(0.105)	0.290
	2	0.097	(3.8)	0.108	(0.104)	0.322
	3	0.076	(3.0)	0.096	(0.092)	0.221
IBT-122	0	0.102	(4.0)	0.092	(0.089)	--
	1	0.119	(4.7)	0.091	(0.088)	0.274
	2	0.122	(4.8)	0.101	(0.097)	0.006
	3	0.107	(4.2)	0.098	(0.094)	0.009
Dual Layer:	0	0.099	(3.9)	.070*	(0.067)	--
IBT-121 - IBT-123	1	0.112	(4.4)	0.070*	(0.067)	0.005*
	2	0.124	(4.9)	0.071*	(0.068)	0.015*
	3	0.094	(3.7)	0.073*	(0.070)	0.010*
Dual Layer:	0	0.061	(2.4)	--		
V-4030 - IBT-123	1	0.064	(2.5)	--		
	2	0.081	(3.2)	--		
	3	0.046	(1.8)	--		
IBT-124	0	0.061	(2.4)	0.111	(0.107)	0.073
	1.5	0.041	(1.6)			

Note: Vacuum level was 1.33×10^{-5} N/cm^2 (10^{-5} torr)

* IBT-123 only

High Vacuum Storage Stability Evaluation of Candidate Advanced Insulation

Figure 21

Propellant/Liner Insulation System	Aging Period	Bond Strength, N/cm^2 (psi) Tensile	Break	Shear	Break
IBT-121/SD-886/ANB-3405-1	0	30 (44)	CI	30 (44)	50 CI/50 CL
	1	57 (83)	CI	20 (29)	F
	2	59 (85)	CI	70 (102)	50 CI/50 CP
	3	66 (96)	CI	61 (88)	50 CI/50 CP
IBT-122/SD-886/ANB-3405-1	0	110 (159)	F	85 (124)	F
	1	119 (172)	F	28 (41)*	F
	2	132 (191)	F	111 (161)	F
	3	44 (64)	F	23 (34)*	F
Dual Layer: IBT-121 and IBT-123/ SD-886/ANB-3405-1	0	63 (92)	CI	50 (73)	FL
	1	98 (142)	CI	63 (92)	CI
	2	31 (45)	CI	46 (67)	CI
	3	54 (79)	CI	50 (73)	CI
Dual Layer: Gen-Gard V-4030-IBT-123/ SD-886/ANB-3405-1	0	89 (129)	CP	80 (116)	CP
	1	124 (180)	F	34 (49)	F
	2	88 (127)	F	114 (165)	F
	3	123 (179)	F	88 (128)	F
IBT-124 /SD-886/ANB-3405-1	0	83 (121)	CP	57 (83)	CP
	1.5	58 (84)	APL	51 (74)	CP

Initial propellant tensile strength 122 N/cm^2, (177 psi)

Break Type:
- CI Cohesive insulation
- CP Cohesive propellant
- CL Cohesive liner
- F Secondary bond failure
- APL Liner-Propellant Interface Separation

120°F Aging Stability Evaluation of
Candidate Advanced Insulation/Liner/Propellant Bond

Figure 22

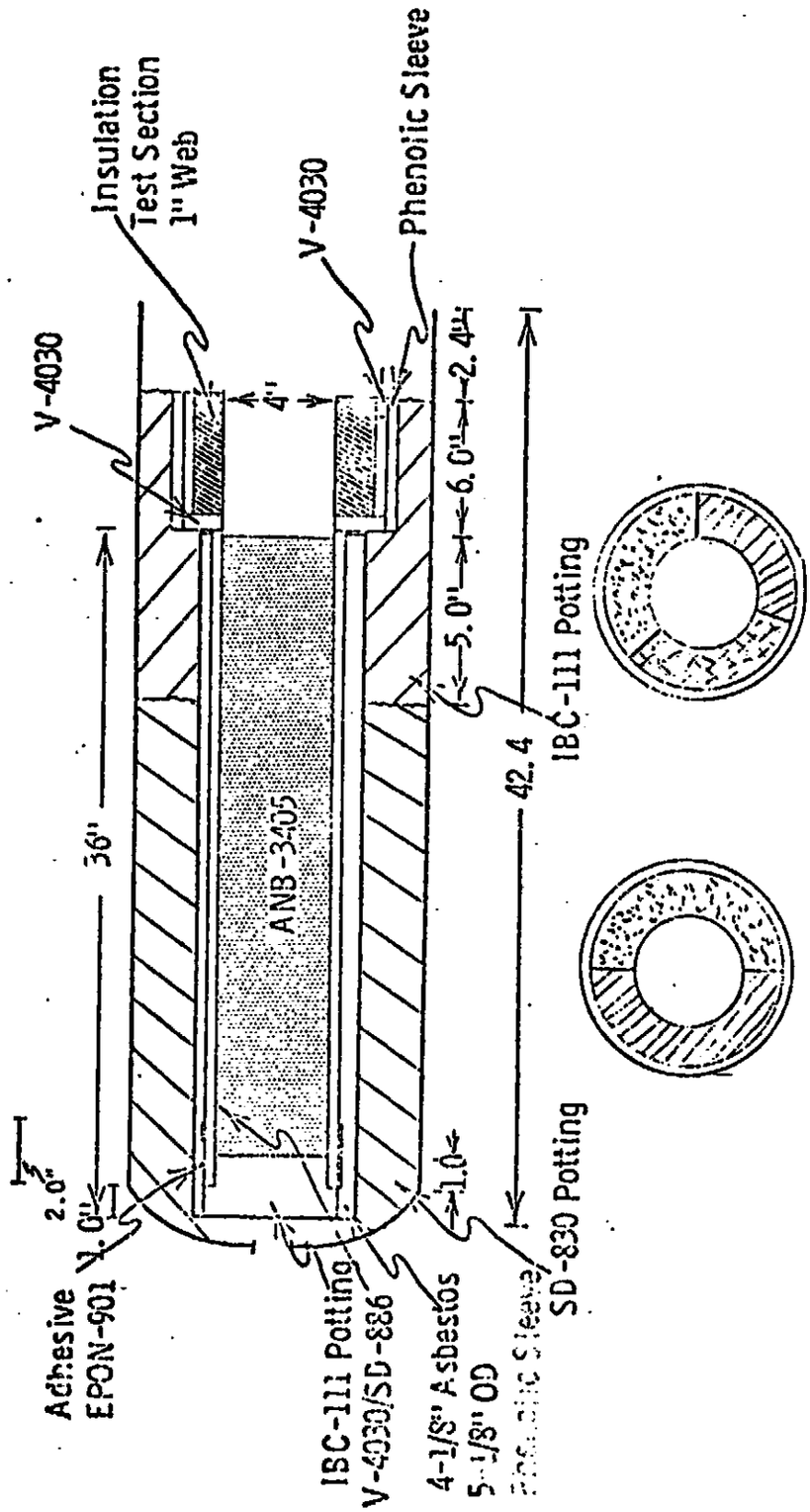

ASPMI End Burning 10KS-2500 Motor

Figure 23

Batch No. 10GP-	Binder Equivalents			Mechanical Properties at 77°F					
	HTPB	TEA	TDI	σ_m N/cm^2	σ_m (psi)	ε_m %	ε_b %	E_o N/cm^2	E_o (psi)
4840	97	3	73	105	(153)	22	25	652	(945)
4841	97	3	70	88.3	(128)	29	33	438	(635)
4842	97	3	67	79.3	(115	34	43	309	(448)

Figure 24

Mechanical Properties of ANB-3405 Propellant

Batch No. 10GP-	Binder Constituents					Infinite Shear Viscosity		Mech. Prop. at 77°F				
	HTPB, eq	TEPAN, Wt%	TEA, eq	TDI, eq	IPDI, eq	poise/hrs	poise/hrs	σ_m N/cm^2	σ_m (psi)	ε_m %	E_o N/cm^2	E_o (psi)
4940	97	-	3	67	-	73,224/2.5	896,994/6.5	79.3	(115)	34	309	(448)
4960	100	0.1	-	-	72	10,170/1.8	23,730/5.8	177	(256)	32	807	(1171)
4961	100	0.1	-	-	75	11,772/2.4	16,350/4.4	185	(268)	25	1035	(1501)
4962	100	0.1	-	-	78	11,554/2.3	15,914/4.3	199	(288)	15	1630	(2364)
4992	100	0.1	-	-	65	-	-	137	(198)	31	557	(808)

ANB-3405 Propellant Data

Figure 25

Ingredient	Weight %
Ammonium Perchlorate, 65/35 SSMP/MA	68.00
Aluminum, Class 2	18.00
Non-plasticized HTPB Binder	14.00
	100.00

Propellant Formulation ANB-3405-1

Figure 26

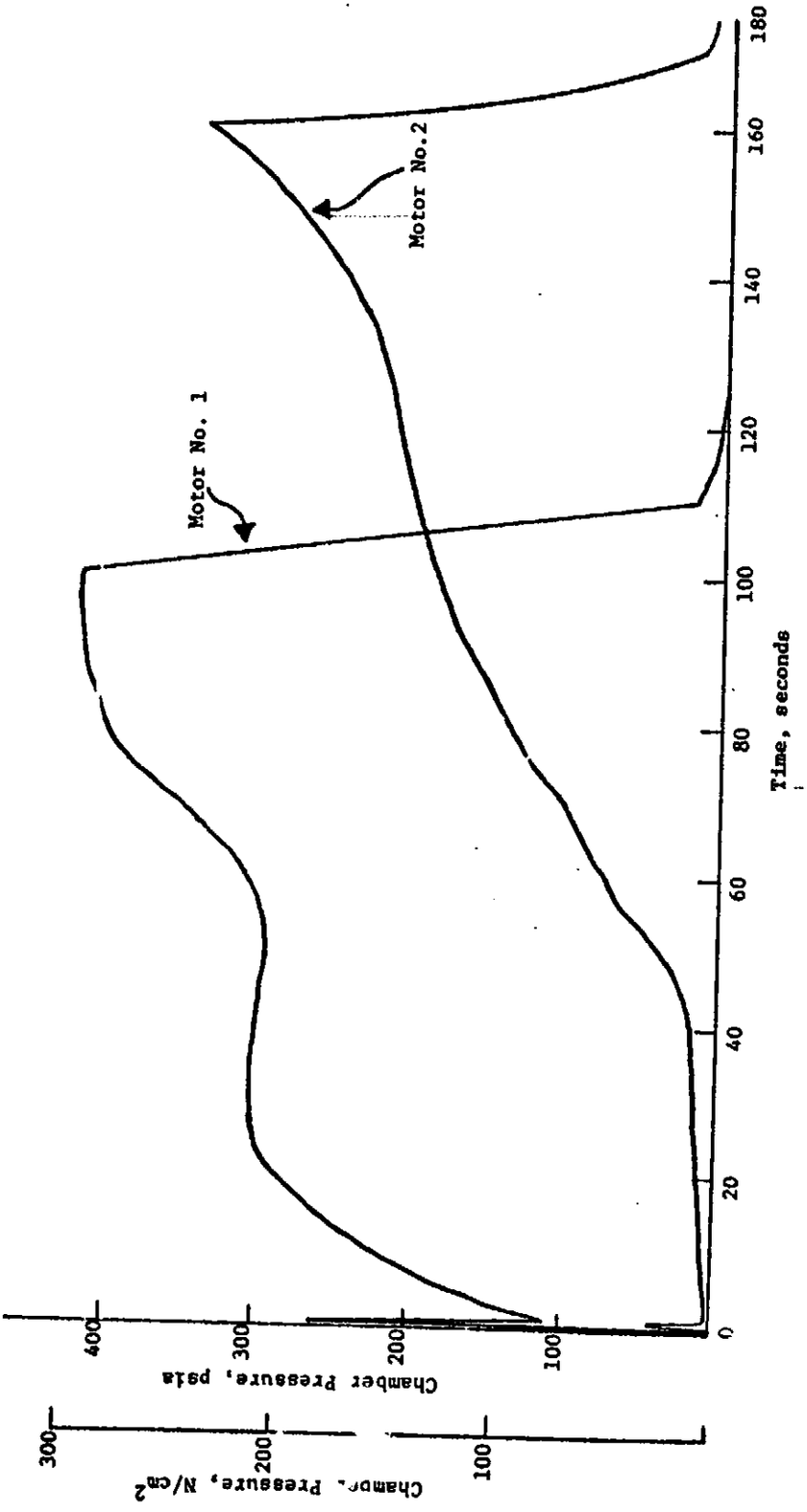

Small-Scale Motor Firings No. 1 and No. 2 Pressure vs Time

Figure 27

Motor Sequence Number	Insulation Systems	Motor Firing Data: Duration, Sec.	Pressure N/cm^2 (psia) Avg	Propellant Burning Rate, cm/sec (in./sec)	Insulation Thickness, cm (in.) Initial	Final	Insulation Ablation Rate, mm/sec (mils/sec)	Mass Flow Rate, N/cm^2 / ($lb/in.^2$ sec) sec.
1	IBT-122	100	218 (316)	0.810 (0.319)	3.188 (1.255)	2.240 (0.882)	0.094 (3.7)	0.0125 (0.0182)
	Gen-Gard V-4030	100	218 (316)	0.810 (0.319)	2.926 (1.152)	2.416 (0.951)	0.051 (2.0)	0.0125 (0.0182)
2	IBT-121	160	97 (141)	0.508 (0.200)	2.954 (1.163)	1.821 (0.717)	0.071 (2.8)	0.0072 (0.0105)
	Gen-Gard V-4030	160	97 (141)	0.508 (0.200)	2.957 (1.164)	2.281 (0.898)	0.043 (1.7)	0.0072 (0.0105)

NOTE. Motors are 10KS-2500 type hardware, see Figure 23.

Figure 28

Small-Scale Motor Firing Data

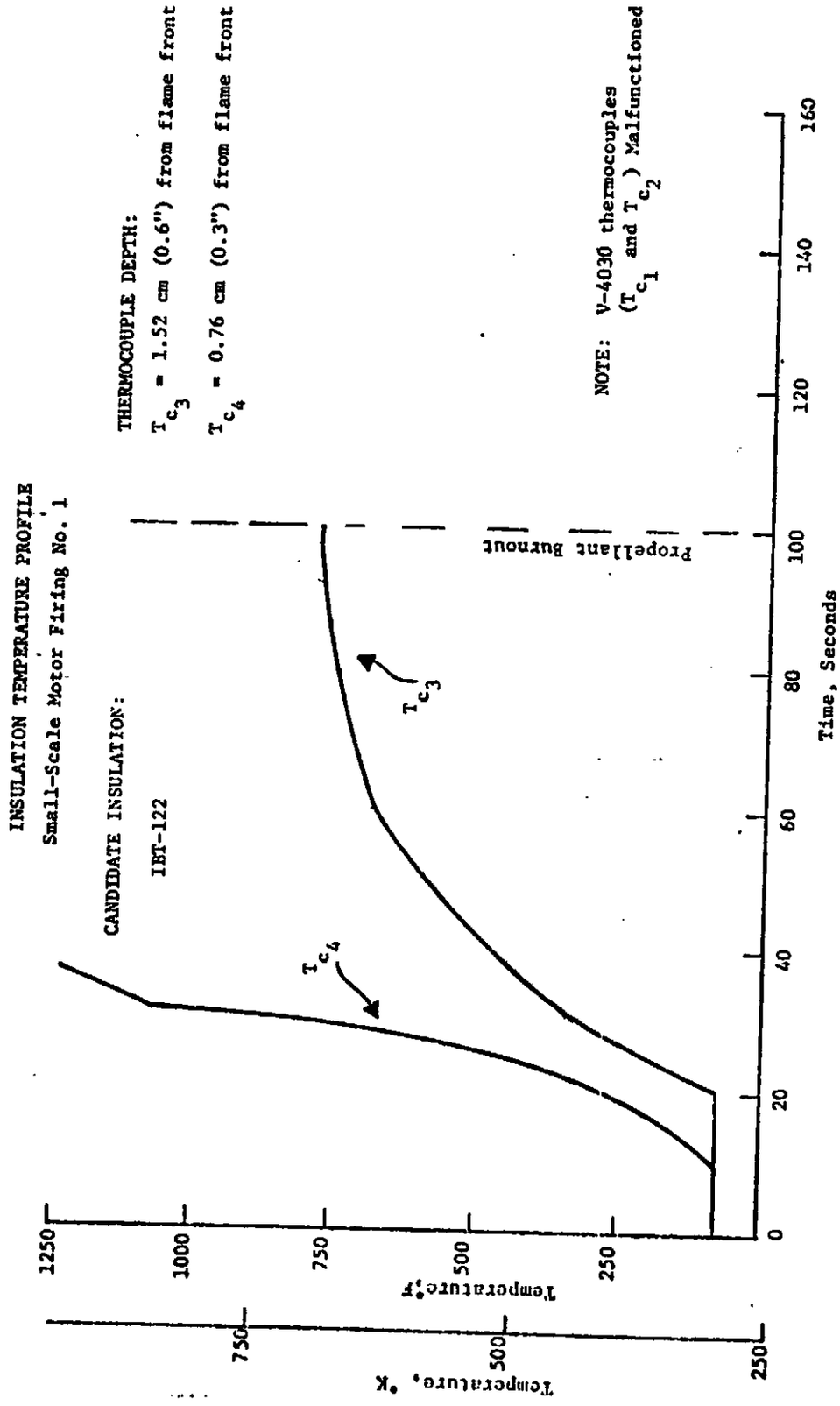

Small-Scale Motor Firing No. 1 Insulation Temperature Profile

Figure 29

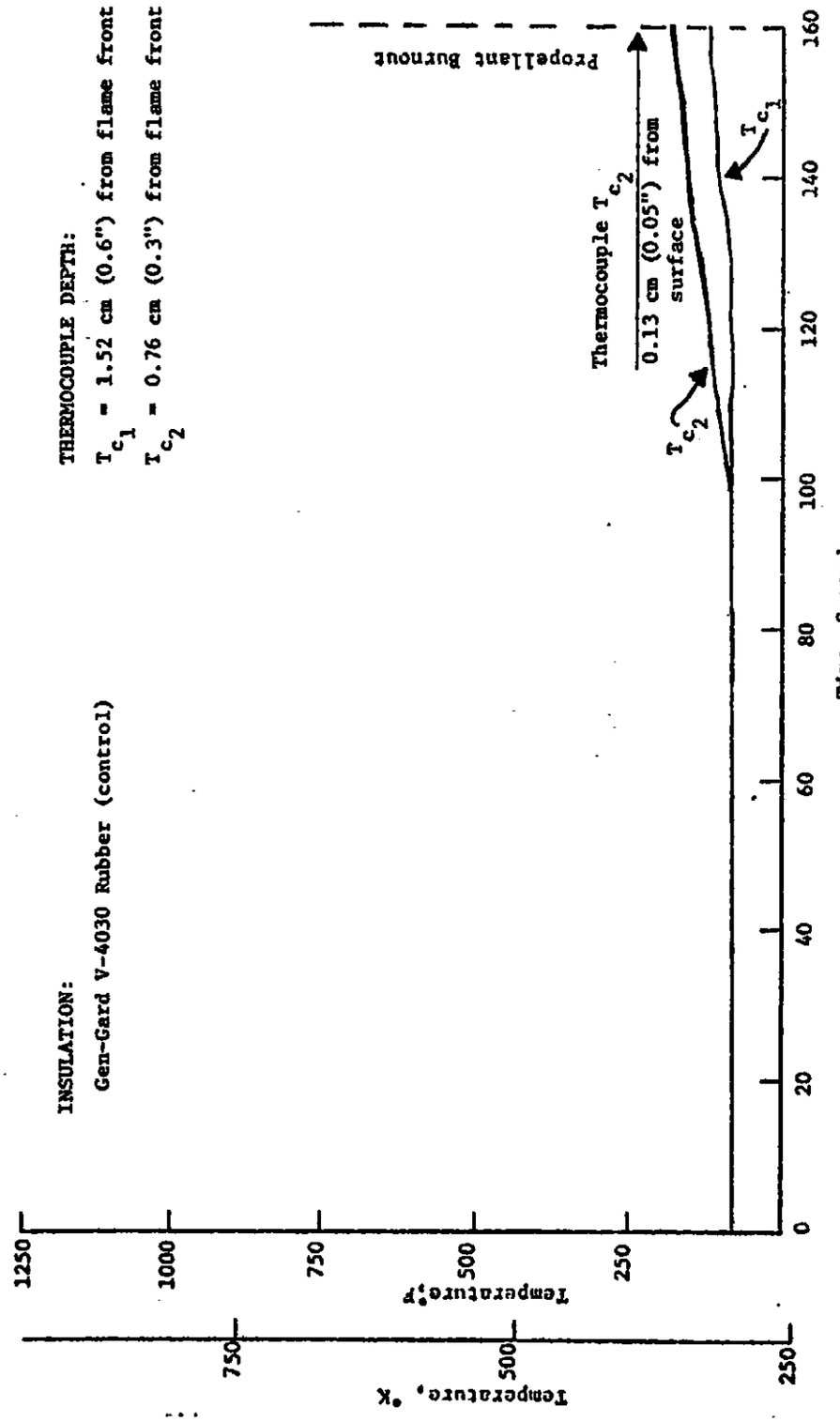

Small-Scale Motor Firing No. 2 Insulation Temperature Profile

Figure 30

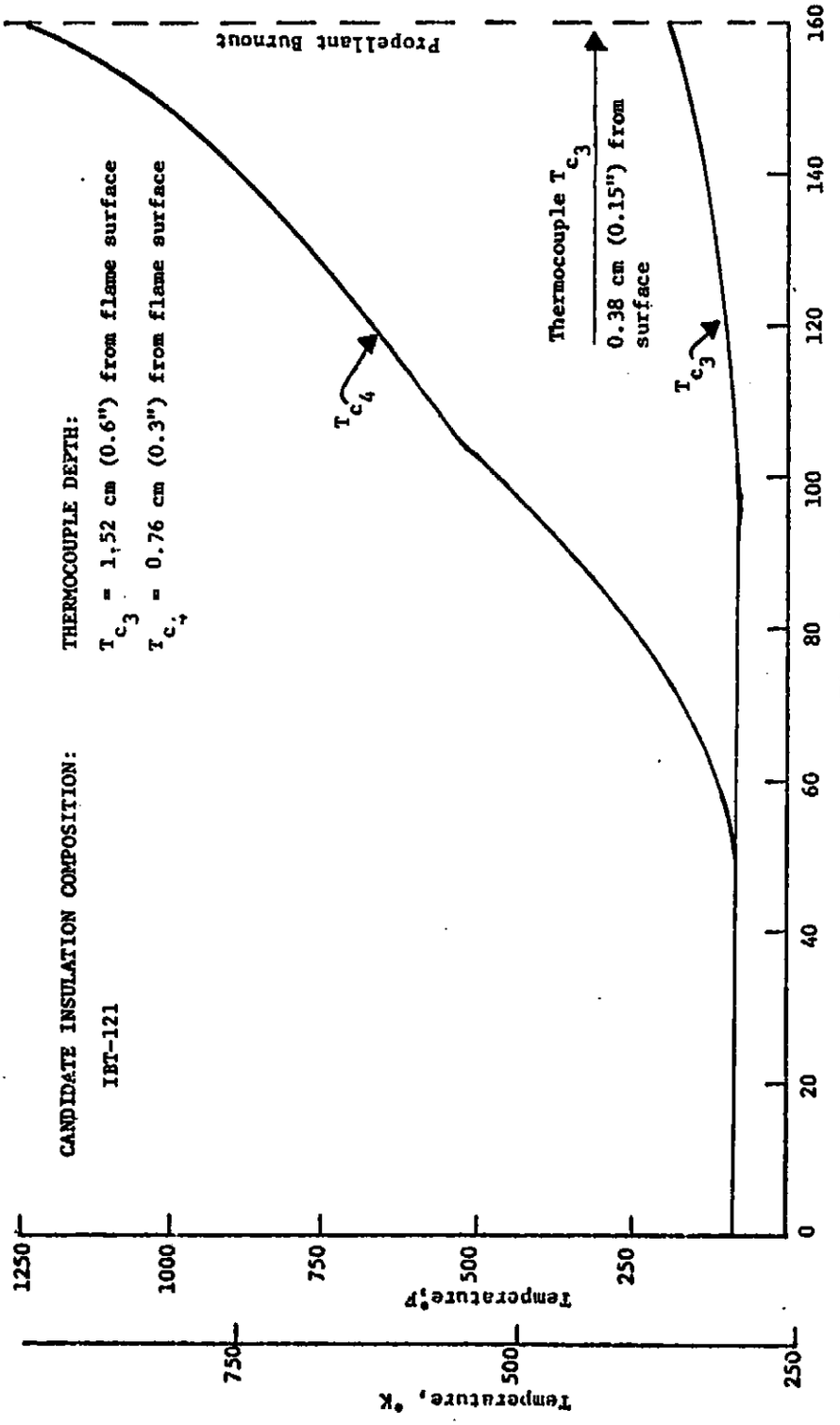

Small-Scale Motor Firing No. 2 Insulation Temperature Profile

Figure 31

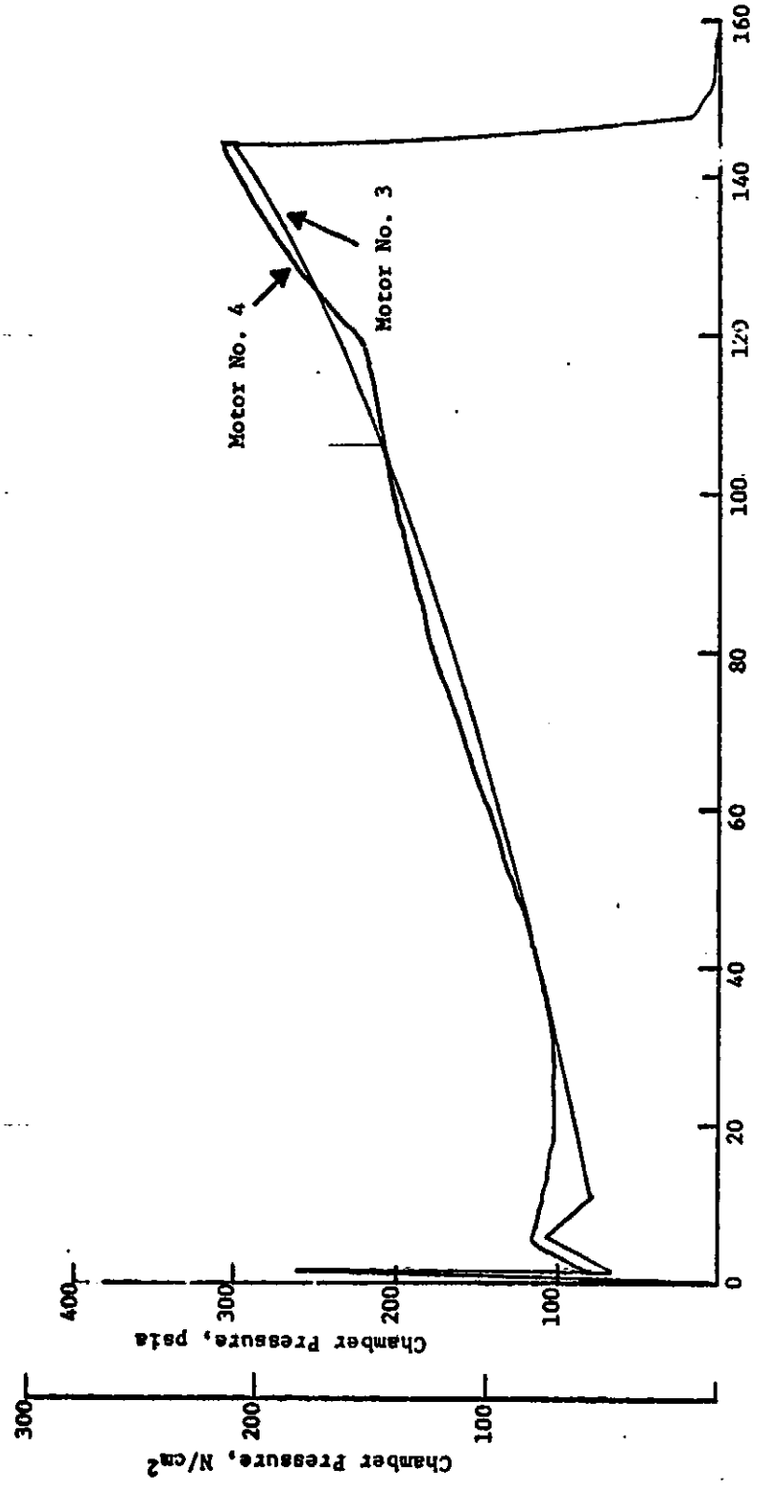

Small-Scale Motor Firings No. 3 and No. 4 Pressure vs Time

Figure 32

Motor Sequence Number	Insulation Systems	Motor Firing Data: Duration, sec.	Pressure, N/cm^2	(psia)	Propellant Burning Rate, cm/sec	(in./sec)	Insulation Thickness, cm (in.) Initial	Final	Insulation Ablation Rate, mm/sec	(mils/sec)	Mass Flow Rate, N/cm^2 / (lb/in.^{2}) sec.	sec)
3	Dual Layer	143.7	121	(176)	0.963	(0.223)			0.099	(3.9)	0.0085	(0.0123)
	Outer Layer: IBT-123						2.192 (0.863)	1.821 (0.717)				
	Inner Layer: IBT-121						0.762 (0.300)	0				
	Gen-Gard V-4030 (control)	143.7	121	(176)	0.963	(0.223)	2.990 (1.177)	2.451 (0.965)	0.038	(1.5)	0.0085	(0.0123)
4	Dual Layer	144.2	117	(169)	0.561	(0.221)			0.056	(2.2)	0.0083	(0.0120)
	Outer Layer: IBT-123						2.423 (0.954)	2.388 (0.940)				
	Inner Layer: Gen-Gard V-4030						0.762 (0.300)	0				
	Gen-Gard V-4030 (control)	144.2	117	(169)	0.561	(0.221)	3.084 (1.214)	2.449 (0.964)	0.043	(1.7)	0.0083	(0.0120)

NOTE: Motors are 10KS-2500 type hardware, see Figure 23.

Figure 33

Small-Scale Motor Firing Data

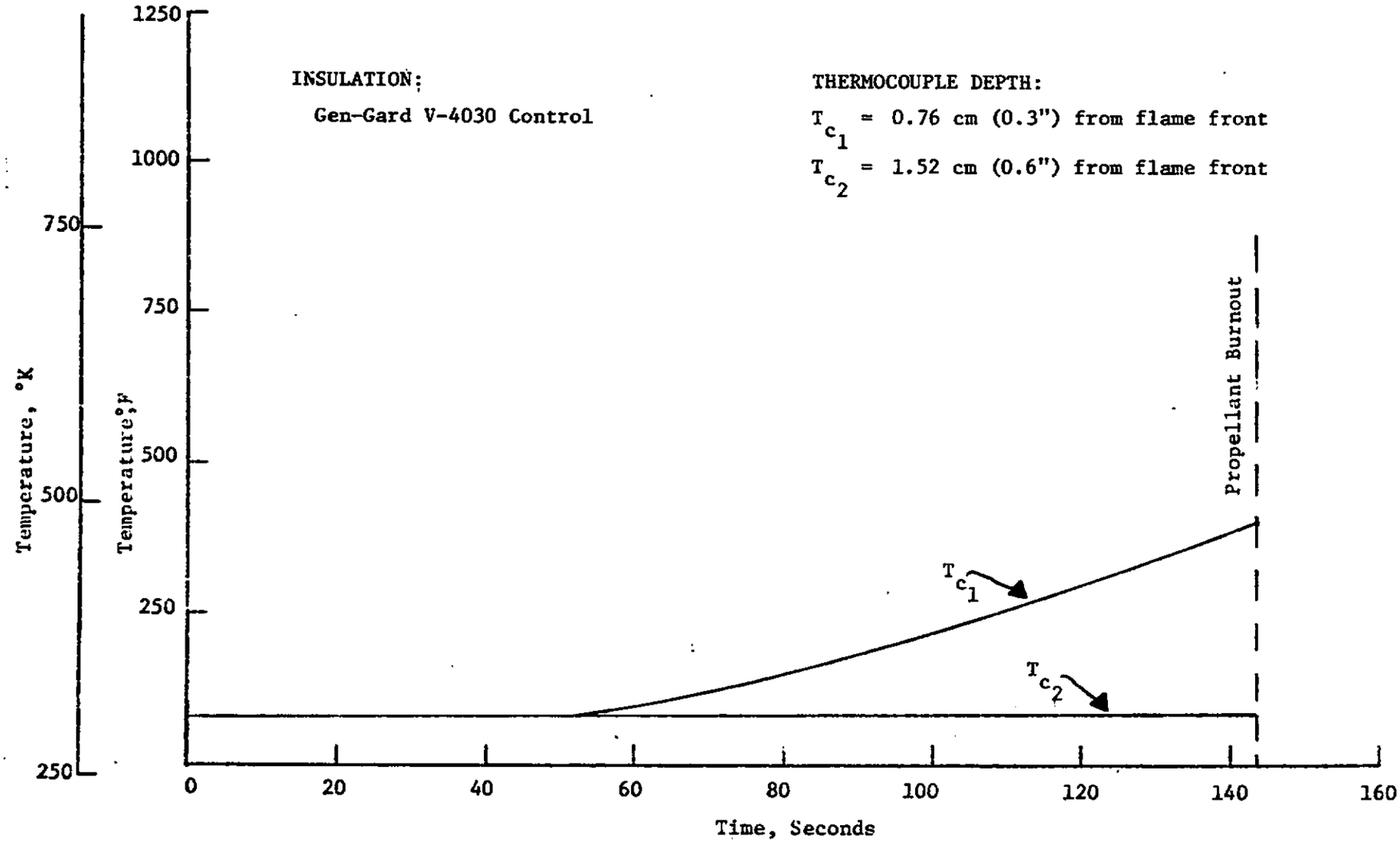

Insulation Temperature Profile, Small-Scale Motor Firing No. 3

Figure 34

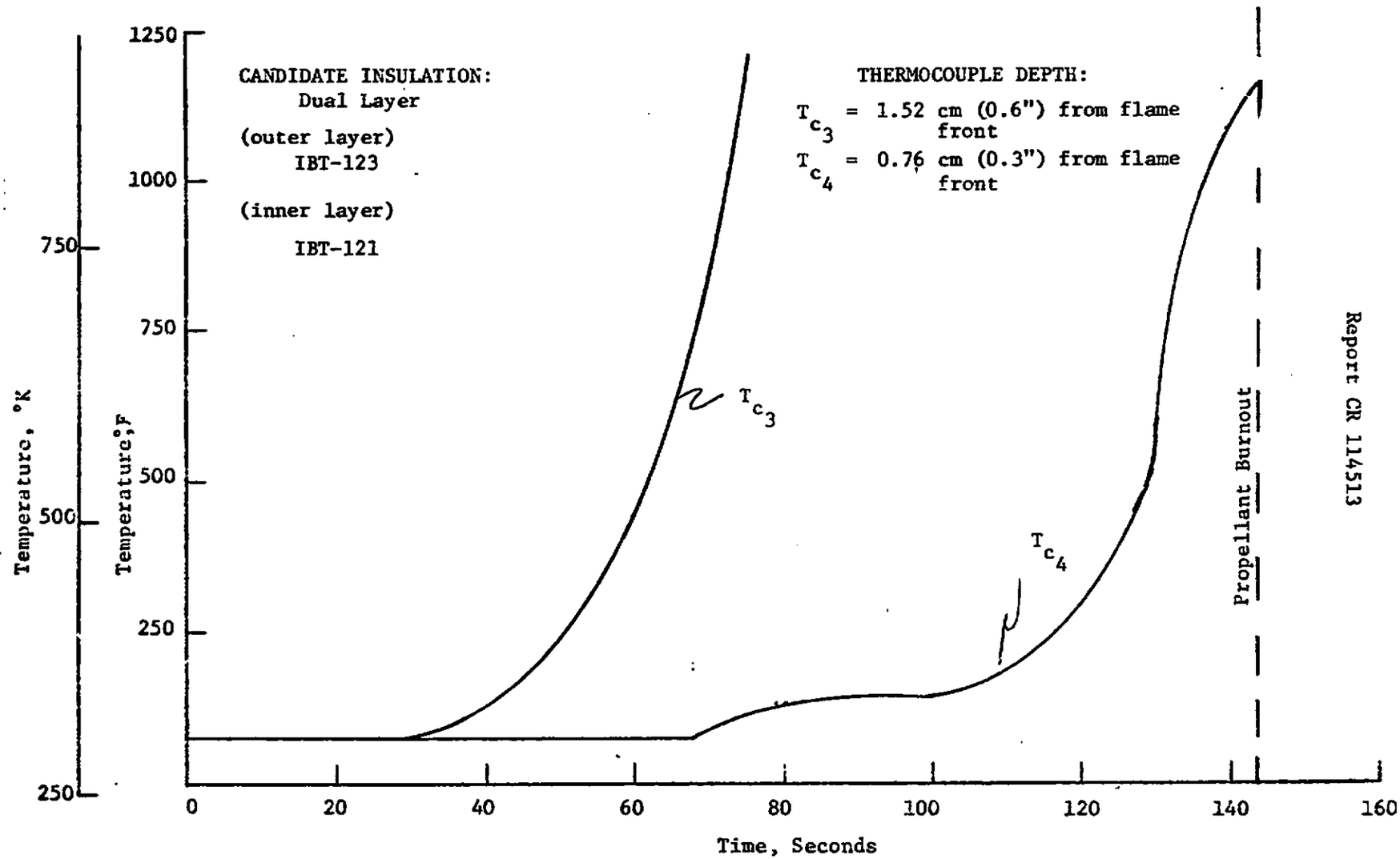

Figure 35

Small-Scale Motor Firing No. 3 Insulation Temperature Profile

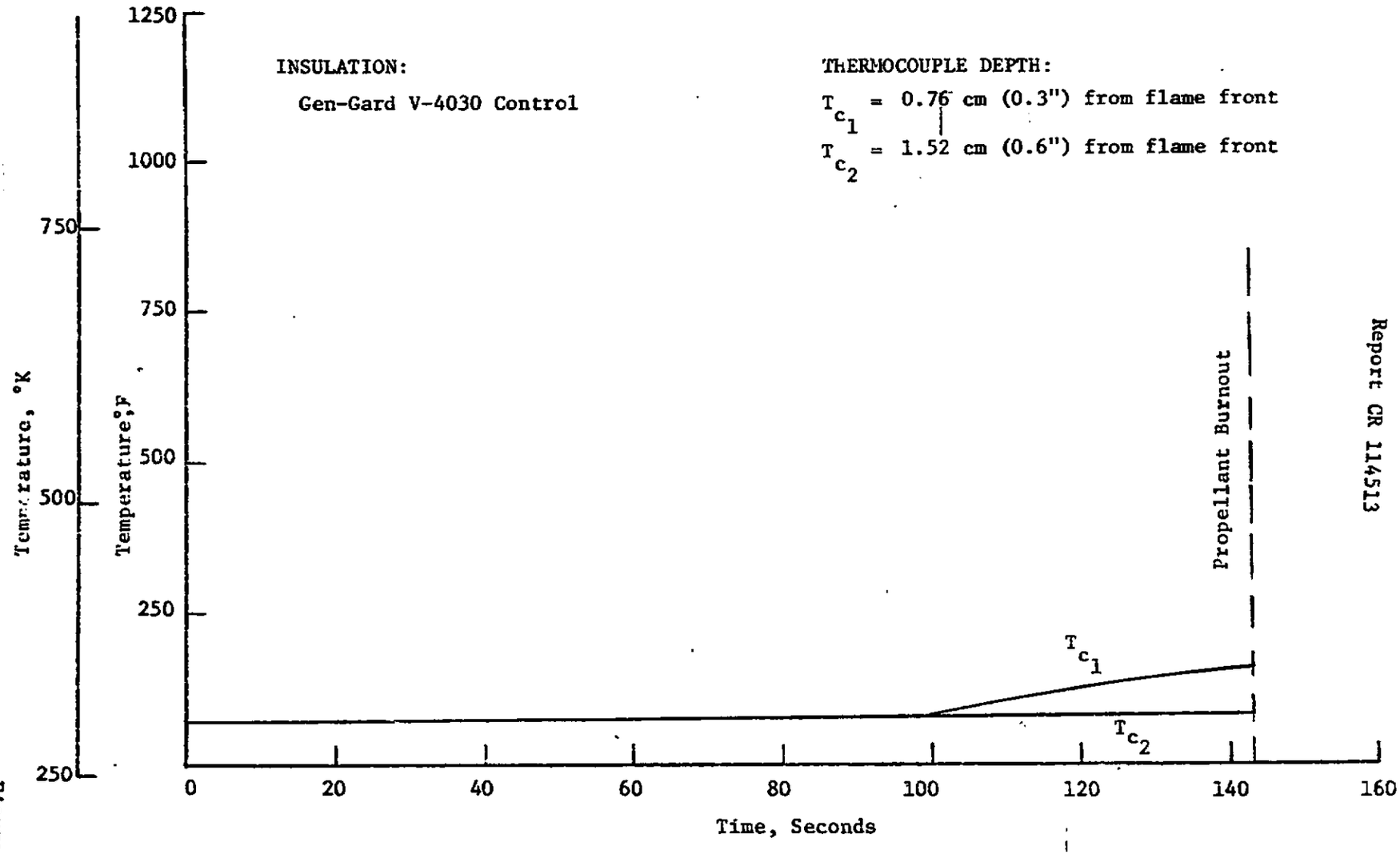

Figure 36

Small-Scale Motor Firing No. 4 Insulation Temperature Profile

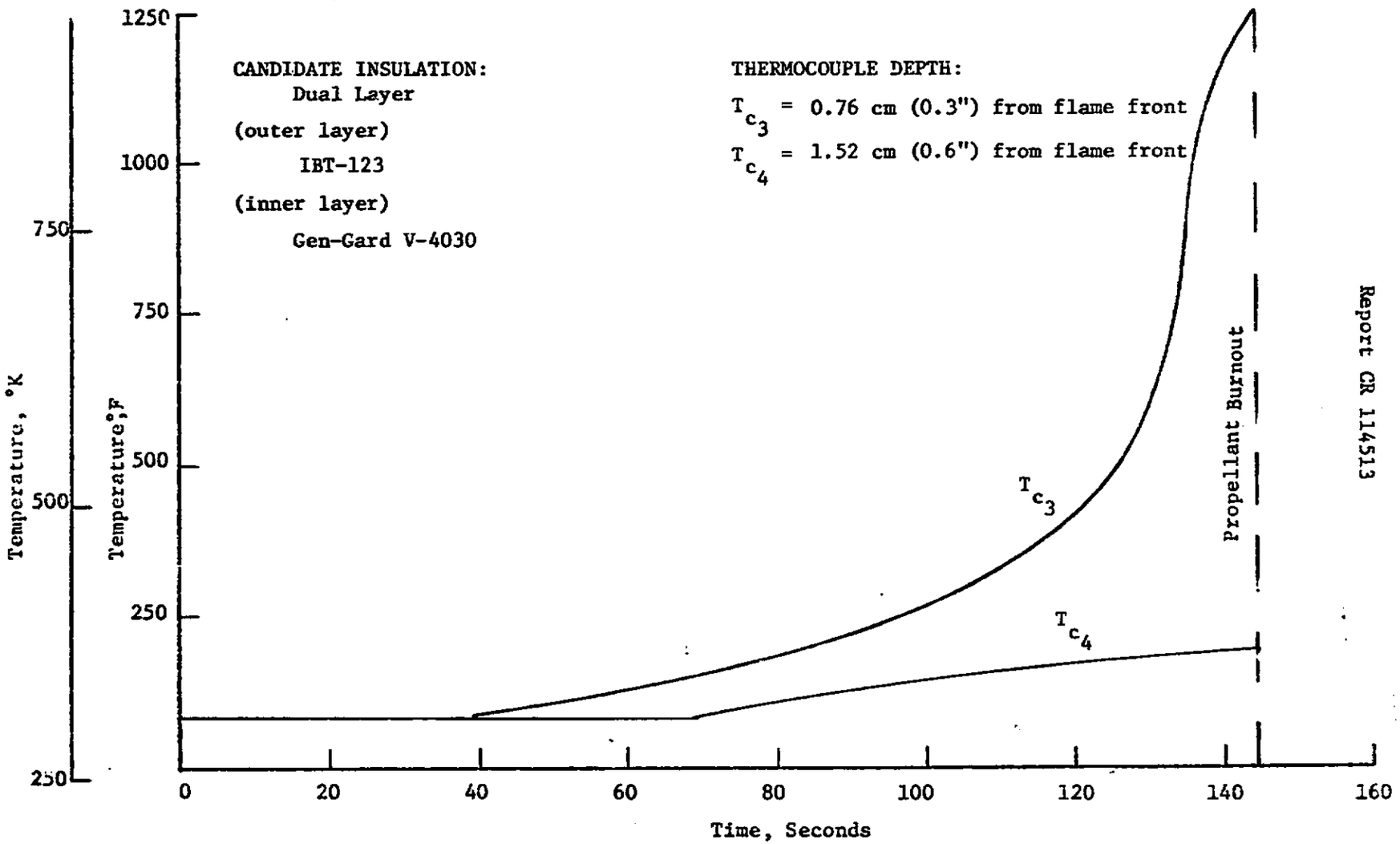

Figure 37

Small-Scale Motor Firing No. 4 Insulation Temperature Profile

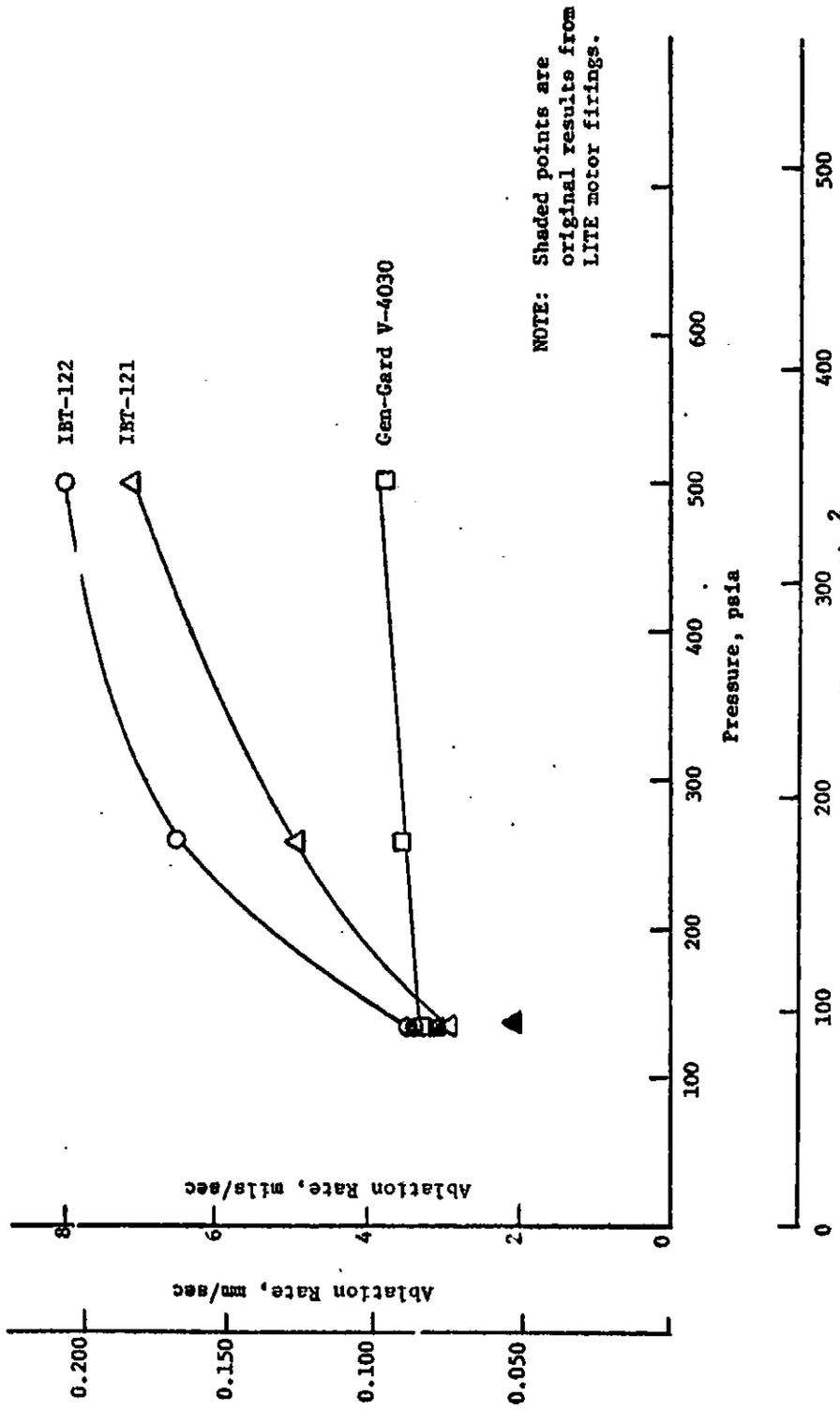

Ablation Rate of Advanced Lightweight Insulation Materials as a Function of Pressure
(LITE Motors)

Figure 38

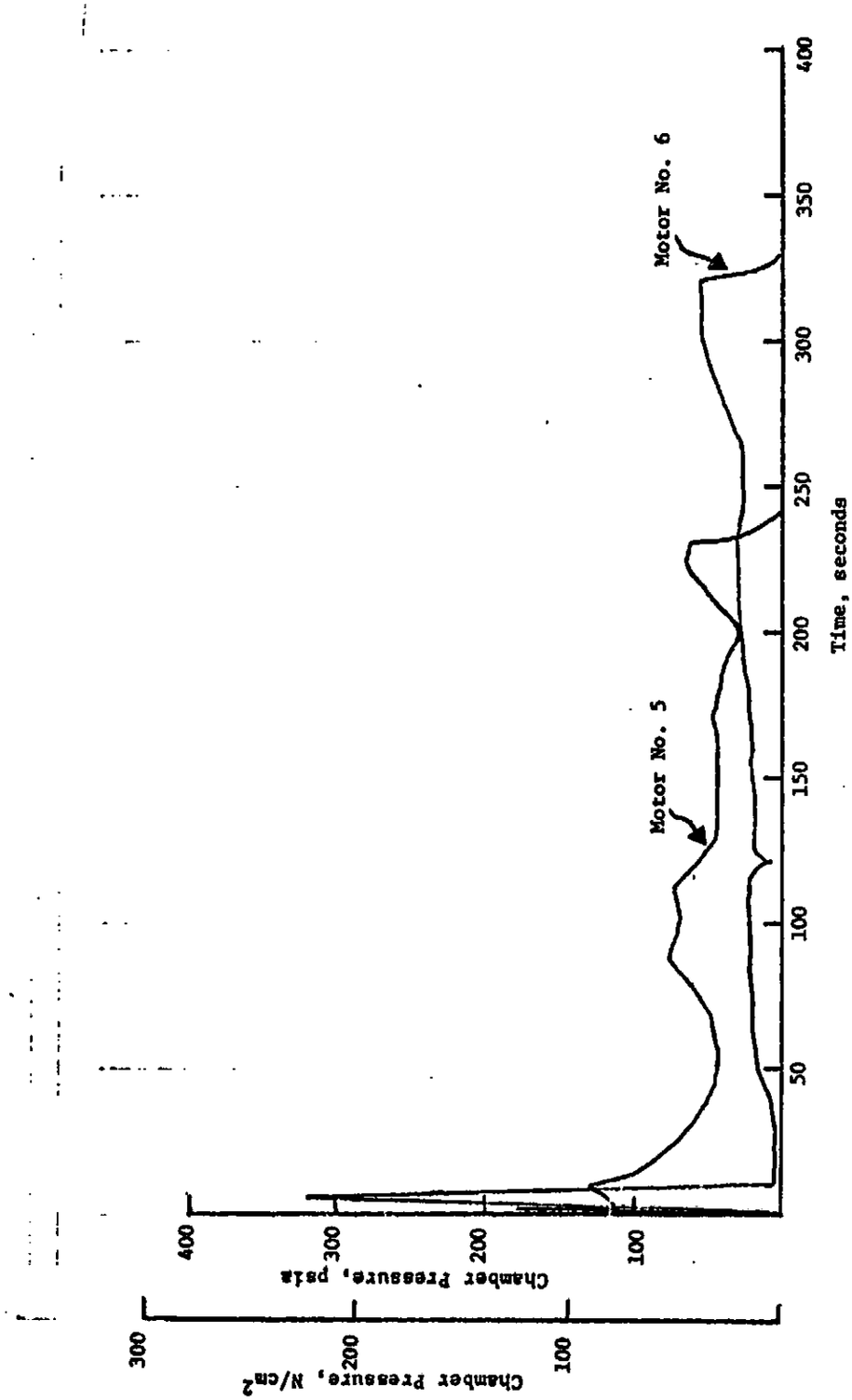

Small Scale Motor Firing No. 5 and No. 6 Pressure vs Time

Figure 39

Motor Sequence Number	Insulation Systems	Motor Firing Data: Duration, sec.	Pressure, N/cm^2 (psia)	Propellant Burning Rate, cm/sec (in./sec)	Insulation Thickness, cm (in.) Initial	Final	Insulation Ablation Rate, mm/sec (mils/sec)	Mass Flow Rate, N/cm^2/(lb/in.^{2} sec) sec.	sec)
5	IBT-121	230	39 (57)	0.353 (0.139)	3.043 (1.198)	1.631 (0.642)	0.061 (2.4)	0.0063	(0.0091)
	IBT-124	230	39 (57)	0.353 (0.139)	3.061 (1.205)	2.449 (0.964)	0.025 (1.0)	0.0063	(0.0091)
	Gen-Gard V-4030 (control)	230	39 (57)	0.353 (0.139)	3.010 (1.185)	2.314 (0.911)	0.030 (1.2)	0.0063	(0.0091)

NOTE: Motors are 10KS-2500 type hardware, see Figure 23.

Figure 40

Small-Scale Motor Firing Data

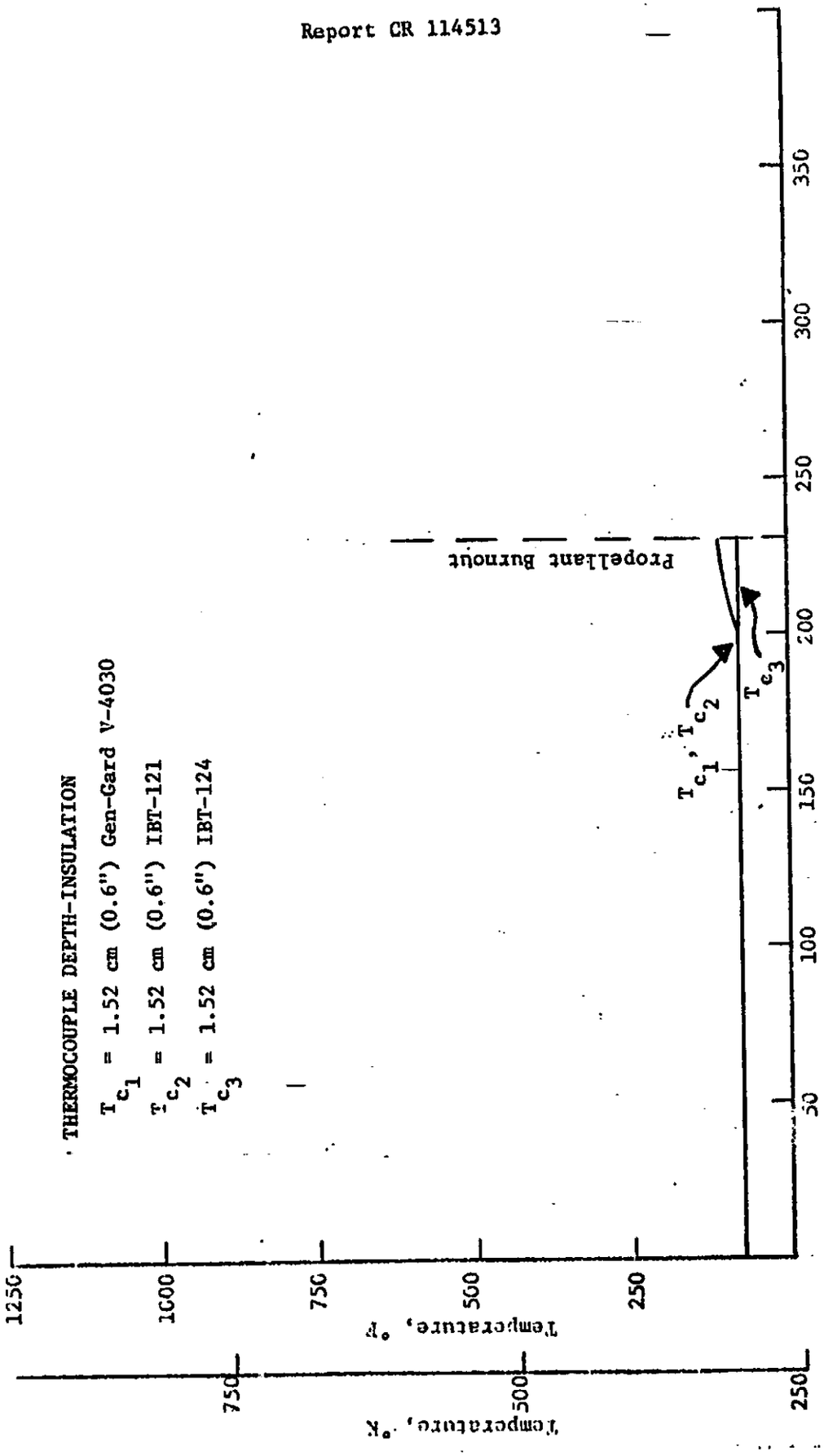

Small-Scale Motor Firing No. 5 Insulation Temperature Profile

Figure 41

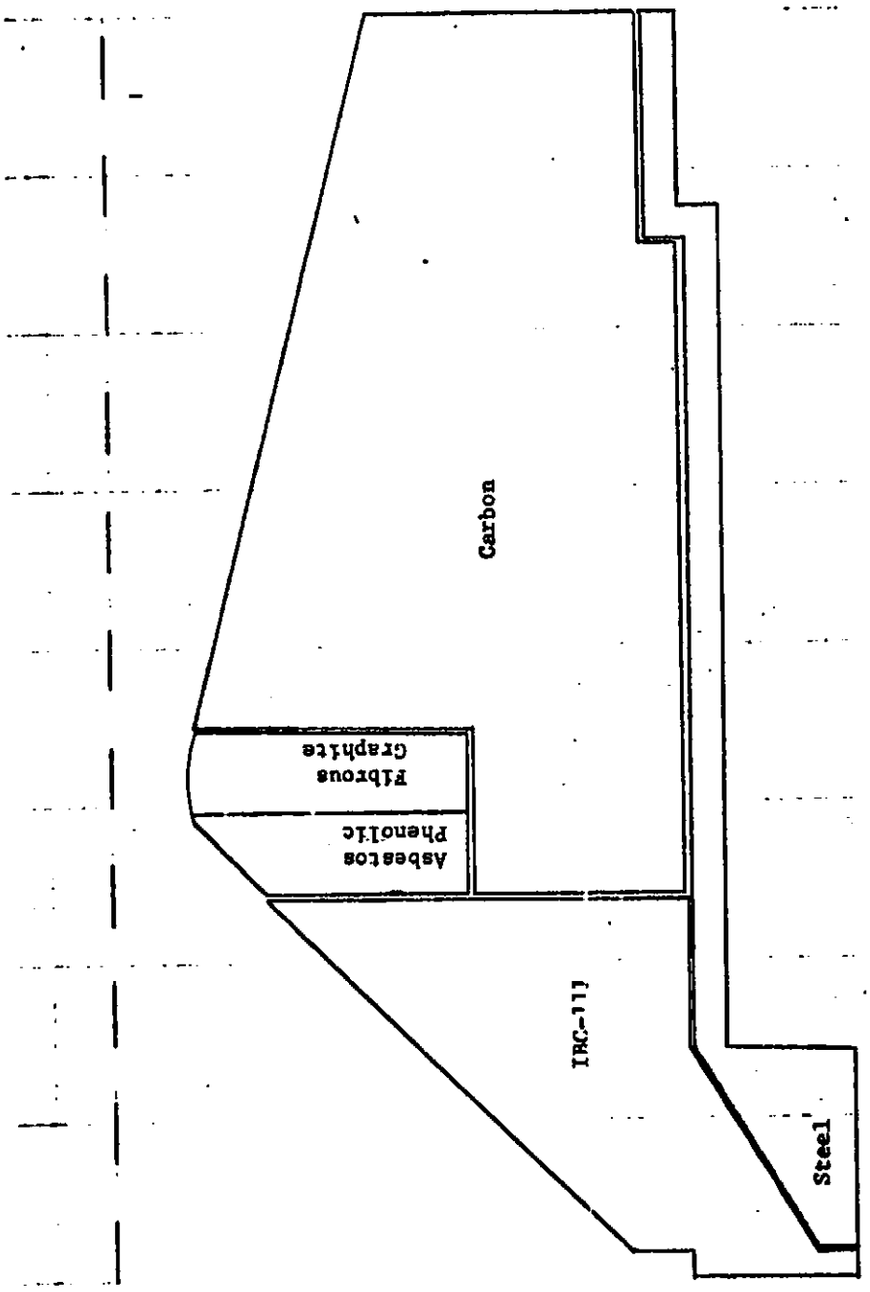

Nozzle Design for Small-Scale Motors No. 7 and No. 8

Figure 42

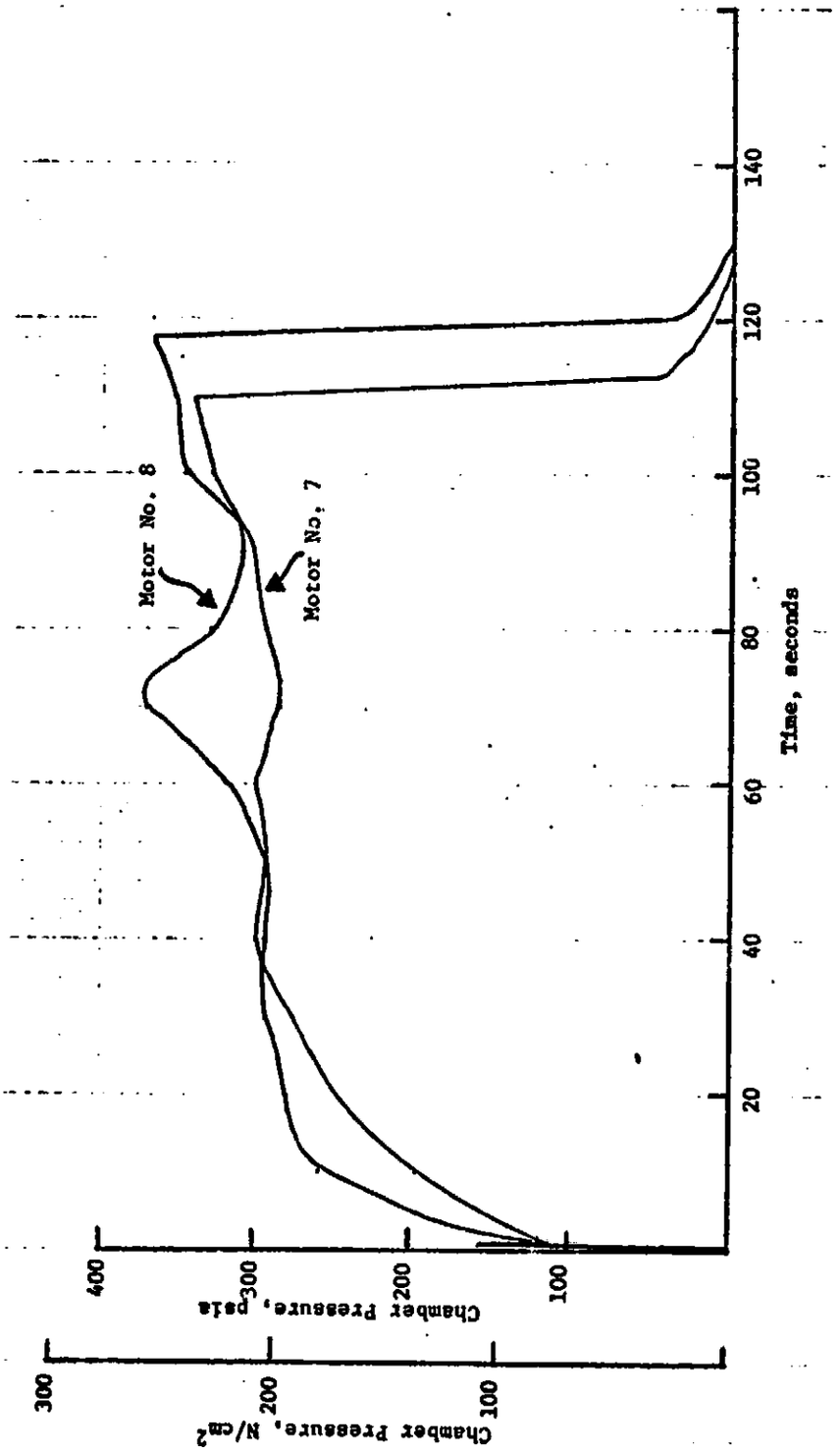

Small-Scale Motor Firings No. 7 and No. 8 Pressure vs Time

Figure 43

Motor Sequence Number	Insulation Systems	Motor Firing Data: Duration Sec	Pressure N/cm²	(psia) Avg	Propellant Burning Rate, cm/sec	(in./sec)	Insulation Thickness, cm (in.) Initial	Final	Insulation Ablation Rate mm/sec	(mils/sec)	Mass Flow Rate N/cm²/sec	(lb/in.²/sec)
7	Dual Layer Gen-Gard V-4030 IBT-123	117.8	196	(284)	0.691	(0.272)	0.762 (0.300) 2.731 (1.075)	0.185 (0.073) 2.731 (1.075)	0.048	(1.9)	0.0133	(0.0193)
	Dual Layer IBT-124/IBT-123	117.8	196	(284)	0.691	(0.272)	0.762 (0.300) 2.679 (1.055)	0.234 (0.092) 2.679 (1.055)	0.046	(1.8)	0.0133	(0.0193)
	Gen-Gard V-4030 (control)	117.8	196	(284)	0.691	(0.272)	3.089 (1.216)	2.527 (0.995)	0.048	(1.9)	0.0133	(0.0193)
8	IBT-122	109.9	027	(300)	0.739	(0.291)	3.025 (1.191)	2.042 (0.804)	0.089	(3.5)	0.0125	(0.0182)
	IBT-124	109.9	207	(300)	0.739	(0.291)	3.272 (1.288)	2.705 (1.065)	0.051	(2.0)	0.0125	(0.0182)
	Gen-Gard V-4030 (control)	109.9	207	(300)	0.739	(0.291)	3.068 (1.208)	2.517 (0.991)	0.051	(2.0)	0.0125	(0.0182)

NOTE: Motors are 10KS-2500 type hardware, see Figure 23

Figure 44

Small-Scale Motor Firing Data

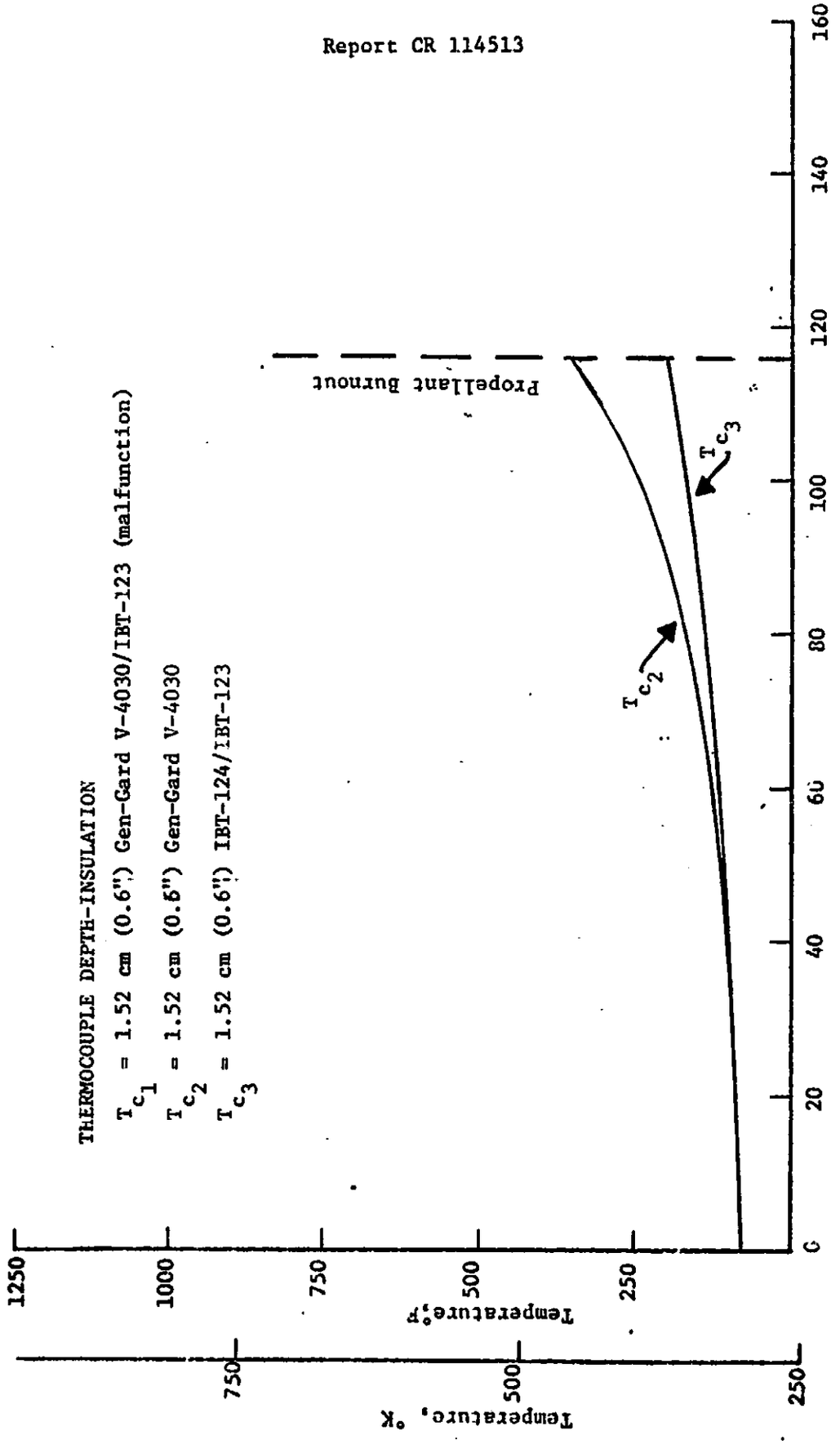

Small-Scale Motor Firing No. 7 Insulation Temperature Profile

Figure 45

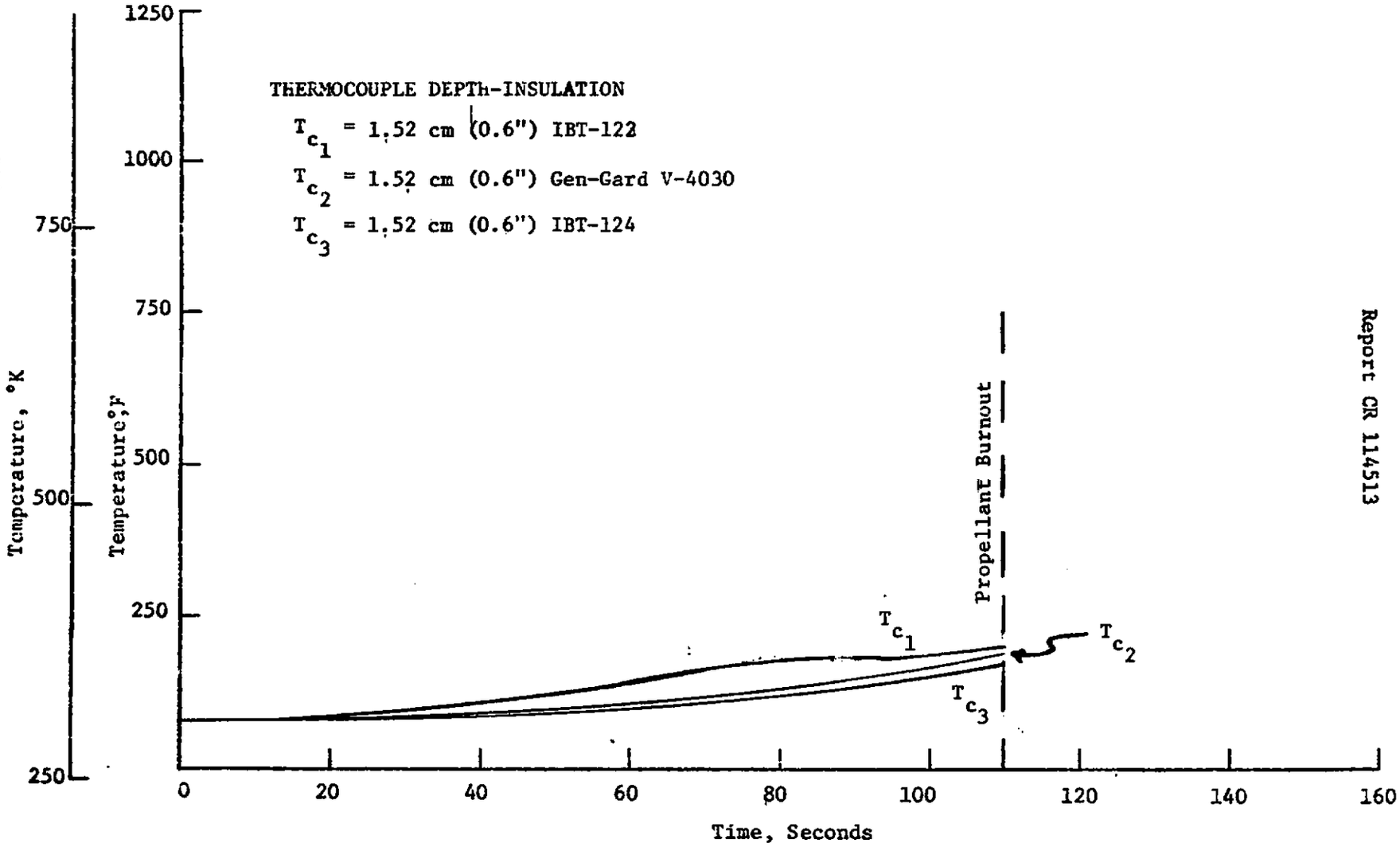

Small-Scale Motor Firing No. 8 Insulation Temperature Profile

Figure 46

Motor	Operating Conditions: Action Time, (sec.)	Operating Conditions: Average Pressure, N/cm^2 (psi)		Material	Average Ablative Rate mm/sec	Average Ablative Rate mils/sec	Temperature Rise at End of Action Time, °K	Temperature Rise at End of Action Time, (°F)
5	230	39	(57)	V-4030	0.030	(1.2)	17	(30)
				IBT-124	0.025	(1.0)	0	(0)
7	117	196	(284)	V-4030	0.048	(1.9)	170	(300)
				IBT-124/IBT-123	0.046	(1.8)	56	(100)
8	110	207	(300)	V-4030	0.051	(2.0)	56	(100)
				IBT-124	0.051	(2.0)	44	(80)

* All temperature rise data were based on thermocouples at a nominal depth of 1.52 cm (0.6 inch).

Figure 47

Comparison of Small-Scale Motor Test Results for IBT-124 and Gen-Gard V-4030

Material	Density Kg/M^3	(lb/ft^3)	Thermal Conductivity J/cm-sec-°K	(BTU/ft Hr °F)	Specific Heat J/gm-°K	(BTU/lb-°F)
V-4030	109	(68)	0.127	(0.122)	1.47	(0.35)
IBT-124	83	(52)	0.104	(0.10)	1.61	(0.385)
IBT-123	55	(34.4)	0.073	(0.07)	1.76	(0.42)

Ablation Model

The thermal analysis employed a charring ablator model which matched the ablation rate characteristics of the IBT-124/IBT-123 composite with those of V-4030.

Figure 48

Thermal Properties of Candidate Insulations and Gen-Gard V-4030

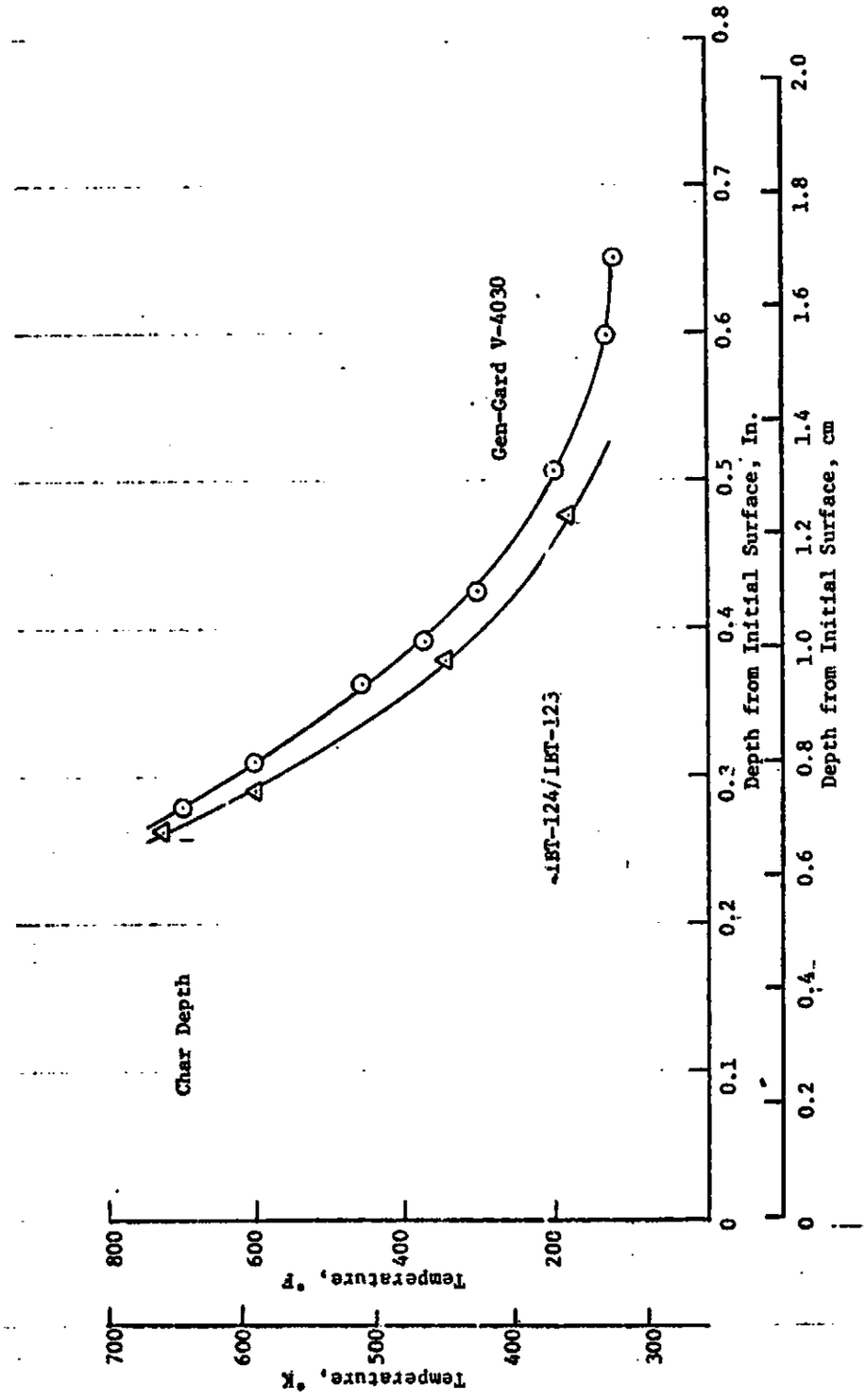

Effect of Insulation Thickness on Case Temperature for Typical Jupiter Orbitor Duty Cycle

Figure 49

IBT-122 Insulation in SVM-2 Chambers

Figure 50

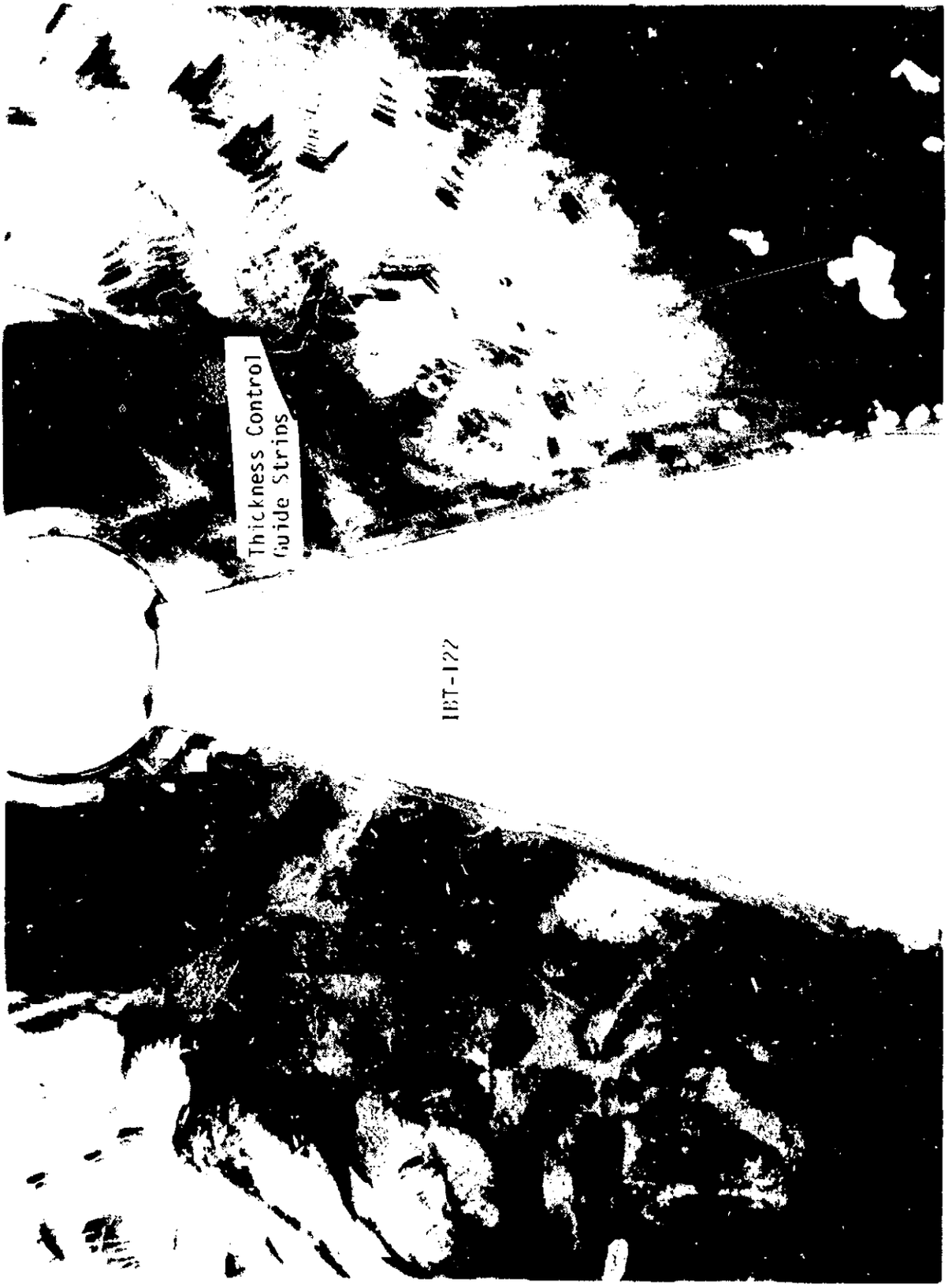

Segment of IBT-122 Insulation Installed in SVM-2 Chamber

Figure 51

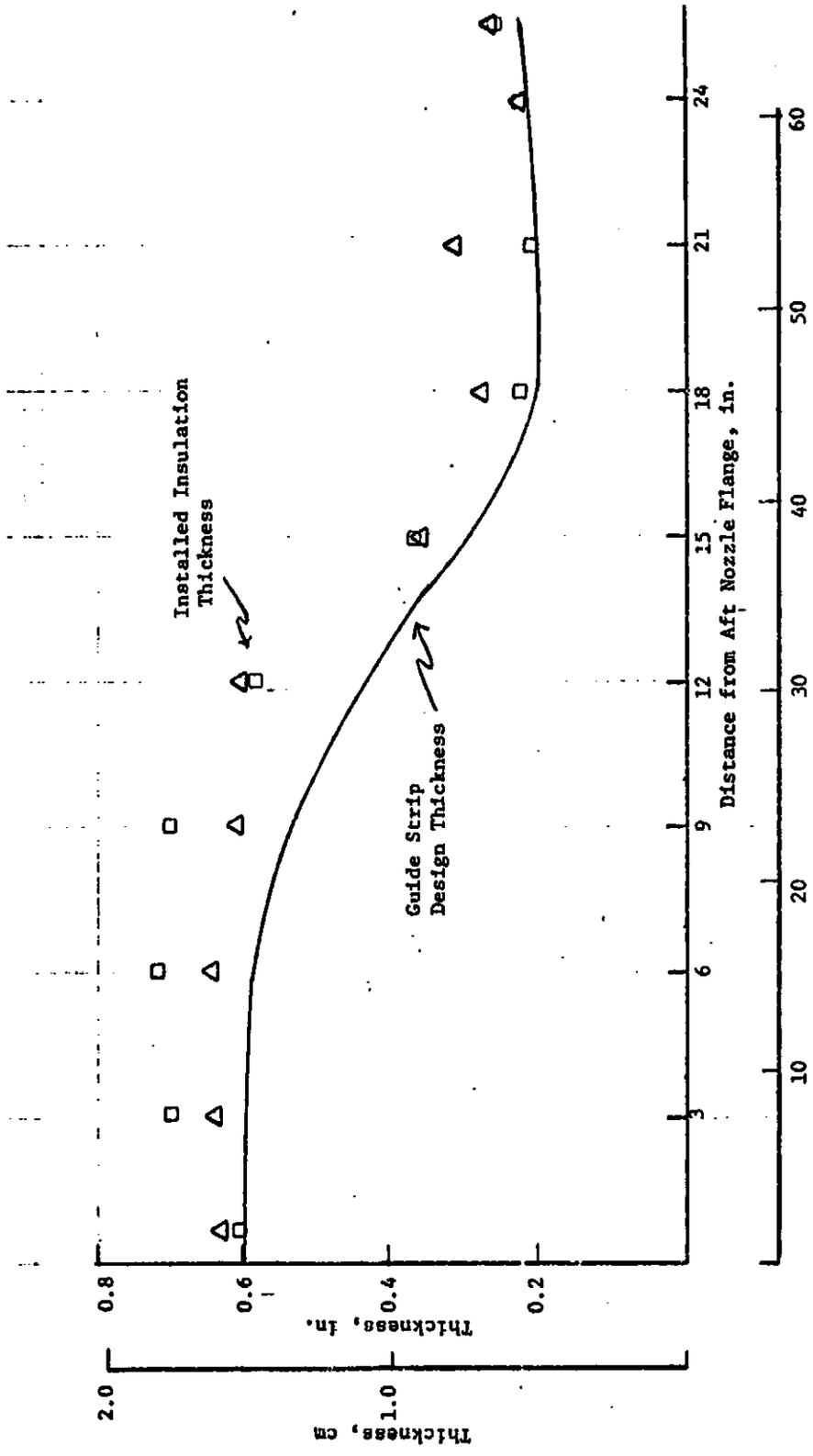

Insulation Thickness Profile, IBT-124

Figure 52